Zurich Open Repository and Archive
University of Zurich
University Library
Strickhofstrasse 39
CH-8057 Zurich
www.zora.uzh.ch

Year: 2017

Rare ADAR and RNASEH2B variants and a type I interferon signature in glioma and prostate carcinoma risk and tumorigenesis

Beyer, Ulrike ; Brand, Frank ; Martens, Helge ; Weder, Julia ; Christians, Arne ; Elyan, Natalie ; Hentschel, Bettina ; Westphal, Manfred ; Schackert, Gabriele ; Pietsch, Torsten ; Hong, Bujung ; Krauss, Joachim K ; Samii, Amir ; Raab, Peter ; Das, Anibh ; Dumitru, Claudia A ; Sandalcioglu, I Erol ; Hakenberg, Oliver W ; Erbersdobler, Andreas ; Lehmann, Ulrich ; Reifenberger, Guido ; Weller, Michael ; Reijns, Martin A M ; Preller, Matthias ; Wiese, Bettina ; Hartmann, Christian ; Weber, Ruthild G

Abstract: In search of novel germline alterations predisposing to tumors, in particular to gliomas, we studied a family with two brothers affected by anaplastic gliomas, and their father and paternal great-uncle diagnosed with prostate carcinoma. In this family, whole-exome sequencing yielded rare, simultaneously heterozygous variants in the Aicardi-Goutières syndrome (AGS) genes ADAR and RNASEH2B co-segregating with the tumor phenotype. AGS is a genetically induced inflammatory disease particularly of the brain, which has not been associated with a consistently increased cancer risk to date. By targeted sequencing, we identified novel ADAR and RNASEH2B variants, and a 3- to 17-fold frequency increase of the AGS mutations ADAR,c.577C>G;p.(P193A) and RNASEH2B,c.529G>A;p.(A177T) in the germline of familial glioma patients as well as in test and validation cohorts of glioblastomas and prostate carcinomas versus ethnicity-matched controls, whereby rare RNASEH2B variants were significantly more frequent in familial glioma patients. Tumors with ADAR or RNASEH2B variants recapitulated features of AGS, such as calcification and increased type I interferon expression. Patients carrying ADAR or RNASEH2B variants showed upregulation of interferon-stimulated gene (ISG) transcripts in peripheral blood as seen in AGS. An increased ISG expression was also induced by ADAR and RNASEH2B variants in tumor cells and was blocked by the JAK inhibitor Ruxolitinib. Our data implicate rare variants in the AGS genes ADAR and RNASEH2B and a type I interferon signature in glioma and prostate carcinoma risk and tumorigenesis, consistent with a genetic basis underlying inflammation-driven malignant transformation in glioma and prostate carcinoma development.

DOI: https://doi.org/10.1007/s00401-017-1774-y

Posted at the Zurich Open Repository and Archive, University of Zurich
ZORA URL: https://doi.org/10.5167/uzh-141037
Journal Article
Accepted Version

Originally published at:
Beyer, Ulrike; Brand, Frank; Martens, Helge; Weder, Julia; Christians, Arne; Elyan, Natalie; Hentschel, Bettina; Westphal, Manfred; Schackert, Gabriele; Pietsch, Torsten; Hong, Bujung; Krauss, Joachim K; Samii, Amir; Raab, Peter; Das, Anibh; Dumitru, Claudia A; Sandalcioglu, I Erol; Hakenberg, Oliver W; Erbersdobler, Andreas; Lehmann, Ulrich; Reifenberger, Guido; Weller, Michael; Reijns, Martin A

M; Preller, Matthias; Wiese, Bettina; Hartmann, Christian; Weber, Ruthild G (2017). Rare ADAR and RNASEH2B variants and a type I interferon signature in glioma and prostate carcinoma risk and tumorigenesis. Acta Neuropathologica, 134(6):905-922.
DOI: https://doi.org/10.1007/s00401-017-1774-y

Acta Neuropathologica

Rare ADAR and RNASEH2B variants and a type I interferon signature in glioma and prostate carcinoma risk and tumorigenesis

--Manuscript Draft--

Manuscript Number:	ANEU-D-17-00473R2
Full Title:	Rare ADAR and RNASEH2B variants and a type I interferon signature in glioma and prostate carcinoma risk and tumorigenesis
Article Type:	Original Paper
Keywords:	Whole-exome sequencing; Aicardi-Goutières syndrome; glioma; prostate carcinoma; type I interferon signaling
Corresponding Author:	Ruthild Gisela Weber Hannover Medical School Hannover, GERMANY
Corresponding Author Secondary Information:	
Corresponding Author's Institution:	Hannover Medical School
Corresponding Author's Secondary Institution:	
First Author:	Ulrike Beyer
First Author Secondary Information:	
Order of Authors:	Ulrike Beyer
	Frank Brand
	Helge Martens
	Julia Weder
	Arne Christians
	Natalie Elyan
	Bettina Hentschel
	Manfred Westphal
	Gabriele Schackert
	Torsten Pietsch
	Bujung Hong
	Joachim K. Krauss
	Amir Samii
	Peter Raab
	Anibh Das
	Claudia A. Dumitru
	I. Erol Sandalcioglu
	Oliver W. Hakenberg
	Andreas Erbersdobler
	Ulrich Lehmann
	Guido Reifenberger
	Michael Weller

Powered by Editorial Manager® and ProduXion Manager® from Aries Systems Corporation

	Martin A. M. Reijns
	Matthias Preller
	Bettina Wiese
	Christian Hartmann
	Ruthild Gisela Weber
Order of Authors Secondary Information:	
Funding Information:	Deutsche Krebshilfe (70-3163-Wi 3) — Not applicable
Abstract:	In search of novel germline alterations predisposing to tumors, in particular to gliomas, we studied a family with two brothers affected by anaplastic gliomas, and their father and paternal great-uncle diagnosed with prostate carcinoma. In this family, whole-exome sequencing yielded rare, simultaneously heterozygous variants in the Aicardi-Goutières syndrome (AGS) genes ADAR and RNASEH2B co-segregating with the tumor phenotype. AGS is a genetically induced inflammatory disease particularly of the brain, which has not been associated with a consistently increased cancer risk to date. By targeted sequencing, we identified novel ADAR and RNASEH2B variants, and a 3- to 17-fold frequency increase of the AGS mutations ADAR,c.577C>G;p.(P193A) and RNASEH2B,c.529G>A;p.(A177T) in the germline of familial glioma patients as well as in test and validation cohorts of glioblastomas and prostate carcinomas versus ethnicity-matched controls, whereby rare RNASEH2B variants were significantly more frequent in familial glioma patients. Tumors with ADAR or RNASEH2B variants recapitulated features of AGS, such as calcification and increased type I interferon expression. Patients carrying ADAR or RNASEH2B variants showed upregulation of interferon-stimulated gene (ISG) transcripts in peripheral blood as seen in AGS. An increased ISG expression was also induced by ADAR and RNASEH2B variants in tumor cells and was blocked by the JAK inhibitor Ruxolitinib. Our data implicate rare variants in the AGS genes ADAR and RNASEH2B and a type I interferon signature in glioma and prostate carcinoma risk and tumorigenesis, consistent with a genetic basis underlying inflammation-driven malignant transformation in glioma and prostate carcinoma development.

Powered by Editorial Manager® and ProduXion Manager® from Aries Systems Corporation

manuscript Click here to download manuscript Beyer et al re-revised.docx

Click here to view linked References

Rare *ADAR* and *RNASEH2B* variants and a type I interferon signature in glioma and prostate carcinoma risk and tumorigenesis

Ulrike Beyer,[1*] Frank Brand,[1*] Helge Martens,[1] Julia Weder,[2] Arne Christians,[3] Natalie Elyan,[1] Bettina Hentschel,[4+] Manfred Westphal,[5+] Gabriele Schackert,[6+] Torsten Pietsch,[7+] Bujung Hong,[8] Joachim K. Krauss,[8] Amir Samii,[9] Peter Raab,[10] Anibh Das,[11] Claudia A. Dumitru,[12] I. Erol Sandalcioglu,[12] Oliver W. Hakenberg,[13] Andreas Erbersdobler,[14] Ulrich Lehmann,[15] Guido Reifenberger,[16,17+] Michael Weller,[18+] Martin A. M. Reijns,[19] Matthias Preller,[2] Bettina Wiese,[20] Christian Hartmann,[3] Ruthild G. Weber[1#]

[1]Department of Human Genetics, Hannover Medical School, Hannover, Germany;
[2]Institute for Biophysical Chemistry, Hannover Medical School, Hannover, and Centre for Structural Systems Biology, Hamburg, Germany;
[3]Division of Neuropathology, Hannover Medical School, Hannover, Germany;
[4]Institute for Medical Informatics, Statistics and Epidemiology, University of Leipzig, Leipzig, Germany;
[5]Department of Neurosurgery, University Medical Center Hamburg-Eppendorf, Hamburg, Germany;
[6]Department of Neurosurgery, Technical University Dresden, Dresden, Germany;
[7]Department of Neuropathology, University of Bonn Medical School, Bonn, Germany;
[8]Department of Neurosurgery, Hannover Medical School, Hannover, Germany;
[9]Department of Neurosurgery, International Neuroscience Institute, Hannover, Germany;
[10]Department of Neuroradiology, Hannover Medical School, Hannover, Germany;
[11]Department of Pediatric Kidney, Liver and Metabolic Diseases, Hannover Medical School, Hannover, Germany;
[12]Department of Neurosurgery, Nordstadt Hospital, Hannover, Germany;
[13]Department of Urology, University of Rostock, Rostock, Germany;
[14]Institute of Pathology, University of Rostock, Rostock, Germany;
[15]Institute of Pathology, Hannover Medical School, Hannover, Germany;
[16]Department of Neuropathology, Heinrich-Heine-University, Düsseldorf, Germany;
[17]German Cancer Consortium (DKTK), partner site Essen/Düsseldorf and German Cancer Research Center (DKFZ), Heidelberg, Germany;
[18]Department of Neurology, University Hospital and University of Zurich, Zurich, Switzerland;
[19]Medical Research Council Human Genetics Unit, MRC Institute of Genetics and Molecular Medicine, University of Edinburgh, Edinburgh, United Kingdom;
[20]Department of Neurology, Henriettenstift, Diakovere Krankenhaus gGmbH, Hannover, Germany.

[*]Ulrike Beyer and Frank Brand contributed equally as first authors to this work.
[+]These authors represent the German Glioma Network.

[#]Correspondence to: Ruthild G. Weber, M.D., Department of Human Genetics OE 6300, Hannover Medical School, Carl-Neuberg-Str. 1, D-30625 Hannover, Germany, Phone: +49 511 5327751, Fax: +49 511 53218520, E-mail: weber.ruthild@mh-hannover.de

Abstract

In search of novel germline alterations predisposing to tumors, in particular to gliomas, we studied a family with two brothers affected by anaplastic gliomas, and their father and paternal great-uncle diagnosed with prostate carcinoma. In this family, whole-exome sequencing yielded rare, simultaneously heterozygous variants in the Aicardi-Goutières syndrome (AGS) genes *ADAR* and *RNASEH2B* co-segregating with the tumor phenotype. AGS is a genetically induced inflammatory disease particularly of the brain, which has not been associated with a consistently increased cancer risk to date. By targeted sequencing, we identified novel *ADAR* and *RNASEH2B* variants, and a 3- to 17-fold frequency increase of the AGS mutations *ADAR,*c.577C>G;p.(P193A) and *RNASEH2B,*c.529G>A;p.(A177T) in the germline of familial glioma patients as well as in test and validation cohorts of glioblastomas and prostate carcinomas versus ethnicity-matched controls, whereby rare *RNASEH2B* variants were significantly more frequent in familial glioma patients. Tumors with *ADAR* or *RNASEH2B* variants recapitulated features of AGS, such as calcification and increased type I interferon expression. Patients carrying *ADAR* or *RNASEH2B* variants showed upregulation of interferon-stimulated gene (ISG) transcripts in peripheral blood as seen in AGS. An increased ISG expression was also induced by *ADAR* and *RNASEH2B* variants in tumor cells and was blocked by the JAK inhibitor Ruxolitinib. Our data implicate rare variants in the AGS genes *ADAR* and *RNASEH2B* and a type I interferon signature in glioma and prostate carcinoma risk and tumorigenesis, consistent with a genetic basis underlying inflammation-driven malignant transformation in glioma and prostate carcinoma development.

Keywords

Whole-exome sequencing; Aicardi-Goutières syndrome; glioma; prostate carcinoma; type I interferon signaling

Introduction

Diffuse gliomas are brain tumors classified by the World Health Organisation (WHO) according to their malignancy, encompassing astrocytomas and oligodendrogliomas of grade II or III, and glioblastomas classified as most malignant grade IV. Most cases of diffuse glioma, as well as of prostate carcinoma occur sporadically. However, familial aggregation of gliomas does exist, accounting for around 5% of patients according to Malmer et al. [43]. Also, glioma susceptibility is increased in patients suffering from certain inherited cancer syndromes, such as neurofibromatosis type 1 and 2, Li-Fraumeni syndrome, and brain tumor polyposis syndromes 1 (Turcot) and 2 (Gardner) (reviewed in [36]), suggesting that genetic alterations play a role in glioma risk. Similarly, familial prostate cancer has been described and tumor syndromes exist that are associated with prostate cancer susceptibility, e.g. Lynch syndrome and hereditary breast and ovarian cancer caused by mutations in DNA-repair genes (reviewed in [41]). Interestingly, genetic alterations in certain genes (e.g. the mismatch repair genes *MSH2*, *MSH6*, *MLH1*, and *PMS2*) or chromosomal regions (e.g. the 8q24 locus) confer increased risk for different tumor entities including gliomas [35, 36] and prostate cancer [4, 41]. Therefore in some families, gliomas and prostate cancer may both be part of a tumor spectrum associated with a common genetic basis. Screening these families for tumor predisposing germline alterations may allow identification of novel genes increasing the risk for these tumor entities, which may also be relevant for sporadic tumor patients. As next generation sequencing technologies have been instrumental in identifying new tumor predisposing genes, such as *POT1* [5] in familial gliomas, we performed whole-exome sequencing in a family with gliomas and prostate carcinomas in four individuals from three consecutive generations. In all affected individuals analyzed, an overlapping data analysis strategy yielded rare, simultaneously heterozygous variants in *ADAR* and *RNASEH2B*, two genes mutated in Aicardi-Goutières syndrome (AGS).

AGS was first described as an infancy onset and rapidly progressive encephalopathy with basal ganglia calcifications and lymphocytosis in the cerebrospinal fluid, reminiscent of an inflammatory process [2]. Presently, AGS is known to be a genetic disorder inherited in an autosomal recessive manner in most cases, and is referred to as a type I interferonopathy

because of a constitutive upregulation of type I interferon (IFN) signaling (reviewed in [18]). The genetic cause of AGS is a mutation in one of seven genes, which encode the three subunits of the ribonuclease H2 (RNase H2) endonuclease complex, RNASEH2A, RNASEH2B and RNASEH2C [17], the 3'-5' DNA exonuclease TREX1 [16], the deoxynucleoside triphosphate triphosphohydrolase and putative exonuclease SAMHD1 [58], the adenosine deaminase acting on RNA ADAR [60], or the cytosolic double-stranded RNA (dsRNA) receptor IFIH1 [59]. ADAR is a dsRNA-editing enzyme that catalyzes the conversion of adenosine to inosine mainly in transcripts expressed in the central nervous system (CNS) [32], and it is an essential suppressor of interferon signaling [27]. RNase H2 cleaves the RNA strand of cellular RNA:DNA hybrids and hydrolyzes ribonucleotides misincorporated into DNA (reviewed in [55]). It is essential for genome stability and mouse embryonic development, with wide-spread DNA damage observed in RNase H2 null cells [30, 56]. RNase H2 deficiency is thought to cause accumulation of cytoplasmic DNA or RNA:DNA resulting from genome instability or endogenous retroviruses, which activate the cGAS-STING innate immune pathway [42, 53].

More generally, accumulation of unprocessed self nucleic acids and subsequent activation of type I IFN signaling are thought to underlie AGS disease pathogenesis. Clinical features include an IFN-stimulated gene (ISG) expression signature as well as inflammation, calcification and neurodegeneration (reviewed in [31]). However, there have also been suggestions that AGS gene variation may be associated with tumorigenesis. Altered ADAR-mediated A-to-I RNA editing was detected in human cancer, whereby global hypoediting described in brain and prostate tumors [50] may be involved in the dedifferentiation of glioma cells [34]. Loss of RNase H2 function was shown to lead to large-scale genomic instability [56], which may be relevant for tumorigenesis. More evidence for an association of AGS and tumor risk comes from an AGS patient carrying a *SAMHD1* germline mutation who developed chronic lymphocytic leukemia (CLL) at 24 years of age [14]. Additionally, somatic *SAMHD1* variants were found in around 10% of relapsed or refractory patients with CLL [14].

In the present study, we present data suggesting that rare partial loss-of-function variants affecting AGS-associated genes *ADAR* and *RNASEH2B* increase the risk for glioma and prostate

carcinoma. Glioma patients carrying *ADAR* and/or *RNASEH2B* mutations and their tumors show signs of a type I interferonopathy. In summary, our data suggest a genetic link between inflammatory processes and the development of glioma and prostate carcinoma.

Materials and methods

Human samples

For the familial glioma cohort (n=60, of these 33 patients were diagnosed with glioblastoma of WHO grade IV), blood samples were collected from glioma patients with evidence for a genetic tumor predisposition because of multiple successive tumors in the glioma patient or tumors in the family history, mainly in Hannover, Lower Saxony, Germany. This cohort includes families 1 and 2. From patient II.2 of family 2, a skin biopsy was performed to obtain fibroblasts. Control fibroblasts were derived from four sex-matched individuals. For the non-familial glioma cohort (n=50, of these 41 patients were diagnosed with glioblastoma), blood samples were collected from glioma patients without multiple successive tumors or family history of tumors in Hannover, Germany. Blood samples from 130 glioma patients diagnosed with *IDH1*-mutant gliomas of WHO grades II or III had been collected in multiple German centers excluding Hannover, and were retrieved from the archives of the German Glioma Network (GGN) (www.gliomnetzwerk.de) [54, 65], which was supported by the German Cancer Aid from 2004 to 2012. Formalin-fixed paraffin-embedded (FFPE) samples from 39 gliomas of WHO grades II or III shown to be *IDH1*-mutant and from 20 glioblastomas (test cohort) were retrieved from the archives of the Department of Neuropathology, Hannover Medical School, Hannover, Germany. The glioblastoma test cohort includes patient II.1 of family 3, whose *RNASEH2B* variant was also detected in non-neoplastic tissue representing the germline. DNA from 56 glioblastomas (validation cohort) was retrieved from the GGN archives. DNA from 15 FFPE prostate carcinoma samples (test cohort) was retrieved from the archives of the Institute of Pathology, Hannover Medical School, Hannover, Germany. The prostate carcinoma test cohort includes patients II.1 of families 4 and 5, whose *ADAR* or *RNASEH2B* variants were also detected in non-neoplastic lymph node representing the

germline. FFPE samples from 50 prostate carcinomas (validation cohort) were retrieved from the archives of the Institute of Pathology, University of Rostock, Rostock, Mecklenburg-Western Pomerania, Germany. All patients provided written informed consent for the use of their tissue samples for research purposes. The study was approved by the Ethics Board of Hannover Medical School, Hannover, Germany, and of the University of Tübingen, Germany.

Whole-exome sequencing (WES)

WES on whole blood DNA from three cancer-affected members of family 1 (patients II.2, III.2, and III.3), and on tumor DNA from the anaplastic glioma of patient III.3 of family 1 was done using the Agilent SureSelectXT All Exon V4 (blood and tumor DNA from patients III.2 and III.3) or V5 (blood DNA from patient II.2) target enrichment kits on an Illumina HiSeq 2000 by Oxford Gene Technology (OGT) [13]. All samples were sequenced to a mean target coverage of >50x. More specifically, on whole blood DNA from patients II.2, III.2, and III.3, average coverage of the *ADAR* coding region was 62x, 96x, and 79x whereby 91%, 88%, and 86% were covered at >25x, while average coverage of the *RNASEH2B* coding region was 60x, 52x, and 39x whereby 77%, 82%, and 66% were covered at >25x. WES germline data were analyzed using INGENUITY Variant Analysis™ (INGENUITY Systems, QIAGEN, Redwood City, USA) and our in-house NGS data analysis workflow as described in Results and Supplementary Tables 1-4. For prediction of variant deleteriousness, the tools SIFT (http://sift.jcvi.org/), PolyPhen-2 (http://genetics.bwh.harvard.edu/pph2/), MutationTaster (http://www.mutationtaster.org), and PROVEAN (http://provean.jcvi.org) were used. Minor allele frequency (MAF) in the European population (non-Finnish) were retrieved from the Exome Aggregation Consortium (ExAC) Browser Beta [39]. Variant verification and co-segregation analysis in families 1 and 2 was done using conventional chain termination protocols on a 3130XL Genetic Analyzer (Applied Biosystems, Darmstadt, Germany). Nucleotide numbering of the identified variants reflects complementary DNA (cDNA) numbering in the GenBank reference sequence. WES tumor data of patient III.3 of family 1 were analyzed with respect to single nucleotide variants and copy number variants within the *ADAR* and *RNASEH2B* loci.

Sequence analysis of *ADAR*, *RNASEH2B*, and SNP rs498872 at 11q23

Whole blood genomic DNA was isolated using QIAamp blood DNA kits (Qiagen, Hilden, Germany). Phenol-chloroform extraction was used to isolate tumor DNA from FFPE tissue. Coding sequences of interferon-induced *ADAR* isoform p150 (NG_011844, NM_001111) or *RNASEH2B* (NG_009055, NM_024570) were amplified using oligonucleotides binding to sequences in close proximity to exon-intron boundaries (Supplementary Tables 5, 6). Using conventional chain termination protocols on a 3130XL Genetic Analyzer, (i) the entire coding regions including splice sites of *ADAR* and *RNASEH2B* were screened for germline mutations in familial glioma patients and patients with *IDH1*-mutant WHO grade II/III gliomas, (ii) the entire coding region including splice sites of *RNASEH2B* as well as *ADAR* exons 2, 5, 8 and 11 were screened for somatic mutations in *IDH1*-mutant gliomas of WHO grade II/III and the glioblastoma and prostate carcinoma test cohort, (iii) hot spot exons, i.e. *ADAR*: exons 2, 5, 8 and 11; *RNASEH2B:* exons 6 and 7, were screened for germline mutations in non-familial glioma patients, and for somatic mutations in the glioblastoma and prostate carcinoma validation cohorts. Genotyping of SNP rs498872 (NM_015157.3:c.-199A>G) located in the 5' UTR of the *PHLDB1* gene at 11q23 was done on germline DNA from patients II.2, III.2, and III.3 of family 1, and patient II.2 of family 2 using conventional chain termination protocols.

Molecular characterization of gliomas

To determine the *IDH1* mutational status, tumor DNA was analyzed using Sanger sequencing or pyrosequencing, or immunohistochemistry using an antibody specifically recognizing the IDH1-R132H mutation was performed on tissue sections [9, 21, 26]. O^6-methylguanine DNA methyltransferase (*MGMT*) promoter methylation was assessed by methylation-specific polymerase chain reaction or pyrosequencing on glioma DNA [20]. The presence or absence of 1p/19q co-deletion was determined by fluorescence *in situ* hybridization using 1p and 19q specific probes on tissue sections or array-CGH of glioma DNA.

Molecular dynamics (MD) simulations

All MD simulations were carried out using NAMD 2.11 [52] and the CHARMM36 force field [7, 25]. Starting coordinates for the duplex Z-DNA-ADAR Zα complex were taken from the crystal structure of human Zα domain with bound Z-DNA (PDB code: 1QBJ). Simulations were performed in explicit solvent using the TIP3P water model [37], and the total charge of each system was neutralized by adding Na^+ counter ions. Each system was initially energy-minimized and subsequently equilibrated for at least 5 ns. MD production runs of each system were conducted for 100 ns at the Computer Cluster of the Norddeutscher Verbund für Hoch- und Höchstleistungsrechnen with periodic boundary conditions in the NpT ensemble at a constant temperature (310 K) and constant pressure (1 atm). A 12 Å cutoff was used for nonbonded short-range interactions and the particle-mesh Ewald method [19] for long-range electrostatics.

Cloning of expression constructs

Human expression constructs pCMV-HA-ADAR p150 (Yanick Crow, University of Manchester, U.K.) and pcDNA3.1-RNASEH2B-Myc/His were described elsewhere [17, 60]. Their ORFs were subcloned into pIRESneo (Matthias Dobbelstein, University of Göttingen, Germany). Murine *Rnaseh2b* ORF was subcloned into pcDNA3.1-Myc vector (Thermo Fisher Scientific, Waltham, MA, U.S.A.). Resulting constructs were used to insert mutations: *ADAR* c.577C>G, *RNASEH2B* c.495G>T or c.529G>A, and *Rnaseh2b* c.486G>T or c.520G>A using the Phusion Site-Directed Mutagenesis® Kit (Thermo Fisher Scientific) according to the manufacturer's instructions. The sequence of all constructs was verified using Sanger sequencing. Oligonucleotide sequences are shown in Supplementary Tables 7, 8.

Cell culture, transfection and stimulation

LN-229, *Rnaseh2b*$^{-/-}$;*Tp53*$^{-/-}$ mouse embryonic fibroblasts (MEFs) [56], and skin biopsy derived primary human fibroblasts were cultured in DMEM (Merck Millipore, Billerica, MA, U.S.A.) supplemented with 10% fetal bovine serum, 2 mM L-glutamine, and 1% penicillin/streptomycin (all Thermo Fisher Scientific). For HCT116 cells, RPMI 1640 (Merck Millipore) was used.

Transient transfection was done using Lipofectamine 3000 reagent (Thermo Fisher Scientific). Stably transfected cell lines were generated by incubation in growth medium supplemented with 600 µg/ml geneticin (Thermo Fisher Scientific) for at least 20 days. Stable *ADAR* expression was verified by PCR amplification of *ADAR* wildtype/mutant inserts using oligonucleotides specifically binding to *ADAR* cDNA sequences. To inhibit JAK1/2 kinases and subsequent JAK/STAT signaling, LN-229 cells were treated with 1 µM of the JAK inhibitor Ruxolitinib dissolved in DMSO versus DMSO control (Selleck Chemicals, Suffolk, UK) for 44h.

Cell proliferation assay

Stably transfected LN-229 or HCT116 cells were seeded in triplicate at a density of 100,000 or 150,000 cells. Cells were counted 9-12 times using the Scepter™ counter (Merck Millipore), and were re-seeded after counting. Growth kinetics were determined for 27 or 28 days, and specific growth rates were calculated. The experiment was repeated once.

Detection of ribonucleotides in genomic DNA

Rnaseh2b$^{+/+}$;*Tp53*$^{-/-}$, *Rnaseh2b*$^{+/-}$;*Tp53*$^{-/-}$, and *Rnaseh2b*$^{-/-}$;*Tp53*$^{-/-}$ MEFs [56] were transiently transfected with *Rnaseh2b* constructs or empty vector and cultured for 48h. MEFs were mechanically disrupted in ice-cold lysis buffer (20 mM Tris-HCl, pH 7.5, 75 mM NaCl, 50 mM EDTA), incubated with 100 µg/ml proteinase K, and completely lysed using sodium dodecyl sulphate at a final concentration of 1%. Nucleic acids were sequentially extracted with TE-equilibrated phenol, phenol:chloroform:isoamylalcohol (25:24:1), and chloroform, precipitated with isopropanol, washed with 75% ethanol, and dissolved in water over night at 4°C. Digestion with RNase HII (NEB, Frankfurt am Main, Germany) was carried out for 1h at 37°C, and nucleic acids were ethanol precipitated and dissolved in water. For alkaline gel electrophoresis [48], one volume of loading buffer (300 mM NaOH, 6 mM EDTA, 7.5% Ficoll (Type 400), 0.35% Orange G) was added to each sample, and DNA was separated on a 0.5% agarose gel (50 mM NaCl, 1mM EDTA) using an alkaline running buffer (50 mM NaOH, 1 mM NaCl) for 16h at 16V (B1 mini-gel format; Thermo Fisher Scientific). After electrophoresis, gels were neutralized with 0.7 M Tris/HCl

buffer (pH 8.0) containing 1.5 M NaCl for 1h at RT and stained with SYBR Gold for 1h at RT (1:10,000 dilution; Thermo Fisher Scientific).

Immunofluorescence staining

Rnaseh2b$^{-/-}$;*Tp53*$^{-/-}$ MEFs transiently transfected with myc-tagged *Rnaseh2b* constructs or vector control expressing RFP, and fibroblasts from patient II.2 of family 2 and controls were fixed with 4% paraformaldehyde, permeabilized with 0.25% Triton X-100, and probed with rabbit anti-phospho-Histone H2AX Ser139 (1:400, #2577, Cell Signaling Technologies, Danvers, MA, U.S.A.). The secondary goat anti-rabbit antibody was Alexa Fluor 488-conjugated (1:500 dilution, A11034, Thermo Fisher Scientific). Transfected MEFs were visualized by co-immunostaining using mouse anti-myc (1:200 dilution, sc-40, Santa Cruz Biotechnology, Dallas, TX, U.S.A.) and Alexa Fluor 568-conjugated goat anti-mouse antibody (1:500 dilution, A10037, Thermo Fisher Scientific). Vector control transfected cells were detected by RFP fluorescence. Cell nuclei were counterstained with DAPI, and analyzed using an epifluorescence microscope (CW4000, Leica Microsystems, Wetzlar, Germany). Cells with more than 5 strong nuclear γH2AX-foci were counted in 100 randomly selected transfected *Rnaseh2b*$^{-/-}$ MEFs [56]. For each patient or control, the number of fibroblasts harboring 0-3 nuclear DNA γH2AX-foci was determined in 50 randomly selected cells (nuclei with more than 3 stress foci were excluded) [23].

LN-229 cells transiently transfected with ADAR or RNASEH2B expression constructs and co-transfected with pEGFP-C1 were fixed with 4% paraformaldehyde, permeabilized with 0.25% Triton X-100, stained with rabbit anti-IRF3 antibody (1:200 dilution, FL-425, Santa Cruz Biotechnology), and a Alexa Fluor 568-conjugated goat anti-rabbit IgG (1:500 dilution; A11011; Thermo Fisher Scientific). For each transfected sample, 200 GFP-positive cells were evaluated semi-quantitatively for their nuclear IRF3 expression level by taking into account the average staining intensity of each visual field and using the scores: no, weak, moderate, or strong.

The co-expression of IFNA6 and GFAP as well as CXCL10 and GFAP was assessed on FFPE glioma sections of patient III.3 of family 1 after heat-induced epitope retrieval in 10 mM citrate buffer pH 6.0, using rabbit anti-IFNA6 (1:100 dilution, HPA047557, Atlas Antibodies) or

rabbit anti-CXCL10 (1:100 dilution, bs-1502R, bioss Center for Biological Signalling Studies, University of Freiburg, Germany), and co-staining with mouse anti-GFAP (1:100 dilution, M0761, Dako, Glostrup, Denmark) as primary antibodies. As secondary antibodies, Alexa Fluor 568-conjugated donkey anti-rabbit IgG (1:300 dilution, A10042, Thermo Fisher Scientific) and DyLight 488-conjugated goat anti-mouse IgG (1:300 dilution, #35503, Thermo Fisher Scientific) were used. Cell nuclei were stained using Hoechst 33342 (Thermo Fisher Scientific).

Assessment of calcification in tissue sections

FFPE glioma and prostate carcinoma sections were hematoxylin eosin (HE) or von Kossa stained and evaluated for visible calcifications using the following score: 1, no detected calcification; 2, one small calcification; 3, several small calcifications; 4, several large calcifications.

Expression analysis of IFNA6, CXCL10, and CD68 by immunohistochemistry

The expression of IFNA6, CXCL10, and CD68 was assessed on FFPE glioma sections after heat-induced epitope retrieval in 10 mM citrate buffer pH 6.0, using rabbit anti-IFNA6 (1:100 dilution, HPA047557, Atlas Antibodies), rabbit anti-CXCL10 (1:300 dilution, bs-1502R, bioss Center for Biological Signalling Studies, University of Freiburg, Germany), and mouse anti-CD68 (1:200 dilution, M 0876, Dako) as primary antibodies. To improve CXCL10 staining, the antibody was diluted in Pierce immunostain enhancer (Thermo Fisher Scientific). As secondary antibody, horseradish-peroxidase-labeled goat anti-rabbit IgG (1:200 dilution, A24537, Thermo Fisher Scientific) was used. Sections were counterstained with hematoxylin (Gill No. 3, 1:10 dilution), scanned using the Aperio AT2 Scanner (Leica Microsystems), and digital images were processed using ImageScope v11.2.0.780 software (Leica Microsystems). On digital images of glioma sections from six patients with and five patients without rare *ADAR* or *RNASEH2B* variants, staining was assessed in six stained, non-overlapping, and non-necrotic areas per section using the following scoring system for staining intensity per area: 0.5, very weak; 1.0, weak; 1.5, moderate; 2.0, moderate to strong; 2.5, strong; 3.0, very strong, and mean staining intensity was calculated for each section.

Expression analysis of interferon stimulated genes (ISG) by real time RT-PCR

The expression of six ISGs, found to be significantly upregulated in AGS patients [60], was assessed in whole blood of male patients III.2 and III.3 of family 1, female patient II.2 of family 2, and 20 controls (10 female and 10 male) matching the sex and age of the three family members. Total RNA was extracted using the PAXgene RNA isolation kit (PreAnalytix, Hombrechtikon, Switzerland). The expression of the three genes found to be upregulated in glioma patients (patients III.2 and III.3 of family 1, patient II.2 of family 2) here was assessed in transiently transfected LN-229 cells that had been treated with 1 µM Ruxolitinib in DMSO or DMSO control. Total RNA was extracted using the RNeasy Mini Kit (Qiagen). cDNA was generated using the Superscript III First-Strand Synthesis System (Thermo Fisher Scientific). Relative quantification was performed using TaqMan Universal PCR Master Mix and TaqMan probes for *IFI27* (Hs01086370_m1), *IFI44L* (Hs00199115_m1), *IFIT1* (Hs00356631_g1), *ISG15* (Hs00192713_m1), *RSAD2* (Hs01057264_m1), and *SIGLEC1* (Hs00988063_m1) (all Thermo Fisher Scientific). Target gene expression levels were normalized to the expression levels of *18S* (Hs999999001_s1) and *HPRT1* (Hs03929096_g1), and comparative C_t quantification was applied. Comparisons between expression levels of the six genes in the patient and the control group were calculated using two-tailed Student's *t* test; multiple testing was corrected for using the Bonferroni-type False Discovery Rate procedure according to Benjamini and Hochberg [6].

Statistics

Data are presented as mean ± SD. Statistical significance was calculated using two-tailed Student's *t* test or Chi Square test, and statistically significant p-values are indicated.

Results

Rare variants in the AGS genes *ADAR* and *RNASEH2B* are associated with glioma and prostate carcinoma risk and tumorigenesis

In family 1, four individuals in three consecutive generations suffered either from *IDH1*-mutant anaplastic astrocytoma of WHO grade III (patients III.2 and III.3) or prostate carcinoma (patients I.1 and II.2). Whole blood derived DNA was available from the two brothers (patients III.2 and III.3) diagnosed with *IDH1*-mutant anaplastic astrocytoma at age 30 and 28 years, respectively, and from their father (patient II.2) affected by a prostate carcinoma (Fig. 1a), and WES was performed. First, to identify variants associated with glioma risk, germline variants shared by the two brothers were analyzed using an overlapping strategy (Supplementary Table 1). Of the shared high-quality variants, 108 were rare (MAF<1%), non-silent (i.e. non-synonymous missense, nonsense, frameshift, and splice site variants), and not found in 56 unrelated in-house controls. Of these variants, 28 fulfilled the following additional criteria: (i) predicted to be deleterious by at least one of four prediction tools, (ii) located within protein domains according to the Uniprot catalog, and (iii) affected genes harbored a second hit (single nucleotide or copy number variant) in the glioma DNA of patient III.3 based on WES data (Supplementary Table 2). A second filtering strategy was applied to the WES data, based on the hypothesis that the prostate carcinomas and the *IDH1*-mutant anaplastic astrocytomas in family 1 were part of a cancer syndrome caused by the same genetic variants. Therefore, germline variants shared by patients II.2, III.2, and III.3 were determined (Supplementary Table 3). Of the shared high-quality variants, 44 were rare (MAF<1%), non-silent (i.e. non-synonymous missense, nonsense, frameshift, and splice site variants), and not found in 56 unrelated in-house controls. Of these variants, nine fulfilled the following additional criteria: (i) predicted to be deleterious by at least one of four prediction tools, (ii) located within protein domains according to the Uniprot catalog, and (iii) affected genes harbored a second hit (single nucleotide or copy number variant) in the glioma DNA of patient III.3 based on WES data (Supplementary Table 4). Manual curation of the 28 variants potentially associated with glioma risk (Supplementary Table 2), and the nine variants potentially associated with glioma/prostate carcinoma risk (Supplementary Table 4) by a clinical

geneticist (RGW) yielded two heterozygous variants in genes associated with the same rare autosomal recessive genetic disorder, AGS: *ADAR,*c.577C>G;p.(P193A), a mutation previously described in AGS patients [60], and *RNASEH2B*,c.495G>T;p.(K165N), a novel missense variant in the AGS gene *RNASEH2B* [17] (Supplementary Tables 9, 10). Verification and segregation analysis by Sanger sequencing in family 1 revealed that only the three family members affected by tumors and from whom DNA was available were simultaneously heterozygous for these *ADAR* and *RNASEH2B* variants, while three cancer-unaffected family members were not (Fig. 1a; Supplementary Fig. 1a). Through WES analysis of DNA derived from the *IDH1*-mutant anaplastic astrocytoma of patient III.3, second hits were detected in the *ADAR* and *RNASEH2B* genes, in addition to the germline missense variants, i.e. a 143 bp deletion partially affecting *ADAR* exon 3, a 286 bp deletion affecting *ADAR* exon 14, and a 225 bp deletion partially affecting *RNASEH2B* exon 1. Tumor DNA from the other two cancer-affected members of family 1 was not available for genetic analysis.

We then determined whether germline variants in *ADAR* and *RNASEH2B* occur at higher than normal frequencies in glioma patients with evidence for a genetic tumor predisposition, either because of multiple successive tumors in the glioma patient or cancer in family members, for whom we use the term familial glioma patients. Targeted sequencing of both genes on germline DNA of 59 additional familial glioma patients was performed. We detected that glioblastoma patient II.2 of family 2 was heterozygous for *RNASEH2B,*c.529G>A;p.(A177T) (Fig. 1b; Supplementary Fig. 1b; Supplementary Tables 9, 10), a variant previously described in AGS patients [17], although the presence of two non-affected heterozygous mutation carriers in family 2 indicates incomplete penetrance for a tumor phenotype (Fig. 1b; Supplementary Fig. 1b). However, the allele frequency for both of the AGS associated variants *ADAR,*c.577C>G;p.(P193A) and *RNASEH2B,*c.529G>A;p.(A177T) was 0.00833 (1 in 120 alleles) in familial glioma patients and, therefore, around 3 and 4 times higher than in non-Finnish Europeans from the ExAC data set [39], i.e. 0.00298 (199 in 66740 alleles) and 0.00193 (128 in 66494 alleles), respectively, and both variants were not found in 263 in-house control exomes. In addition, a novel *RNASEH2B* variant was detected (Supplementary Table 9). Taken together, the

frequency of all rare (MAF<1%) non-silent deleterious *RNASEH2B* variants (that is, frameshift, stop gained/lost, canonical splice site, and initiation codon variants, as well as missense variants predicted to be deleterious by either SIFT or PolyPhen-2 prediction tools and not detected homozygously) in our unrelated familial glioma patients was significantly higher (2 families with multiple variant carriers in 60 families, 3.33%) than in (i) non-Finnish Europeans from the ExAC data set (243 variant carriers in 33,370 individuals, 0.73%) (two-tailed p-value=0.0181, Chi square test), and (ii) in-house control exomes (0 variant carriers in 263 individuals, 0%) (two-tailed p-value=0.0340, Fisher's exact test). No frequency comparison with control data sets was done for variation in *ADAR* because rare deleterious *ADAR* variants were not recurrently detected in our 60 familial glioma patients. No rare non-silent variants in *ADAR* or *RNASEH2B* were detected in the germline of 180 non-familial glioma patients, i.e. without multiple successive tumors or cancer in family members, including 130 patients affected by *IDH1*-mutant gliomas of WHO grade II or III, similar to patients III.2 and III.3 of family 1 found to be simultaneously heterozygous for *ADAR* and *RNASEH2B* variants (Supplementary Table 9). Because SNP rs498872 at 11q23 is one of the variants reported to specifically increase the risk for *IDH1*-mutant glioma [61], we assessed this variant on germline DNA from tumor-affected members of families 1 and 2. While patient II.2 of family 1 diagnosed with prostate cancer was heterozygous for the risk allele (NM_015157.3:c.-199A>G), none of the patients affected by *IDH1*-mutant or *IDH1*-wildtype gliomas carried the risk allele (Supplementary Fig. 2). Therefore, the risk allele at 11q23 was not associated with the susceptibility for *IDH1*-mutant glioma in family 1.

Targeted *ADAR* and *RNASEH2B* sequencing was also performed on tumor-DNA from all three tumor types found in patients carrying rare *ADAR* or *RNASEH2B* germline variants, i.e. *IDH1*-mutant gliomas of WHO grade II/III, glioblastomas (on geographically distinct test and validation cohorts), and prostate carcinomas (on geographically distinct test and validation cohorts). While no rare non-silent somatic *ADAR* or *RNASEH2B* variants were found in 39 *IDH1*-mutant gliomas of WHO grade II/III, the allele frequency for the known AGS variant *RNASEH2B,*c.529G>A;p.(A177T) was 0.025 (1 in 40 alleles), i.e. 13 times higher, in a glioblastoma test cohort, and that of *ADAR,*c.577C>G;p.(P193A) was 0.00893 (1 in 112 alleles),

i.e. 3 times higher, in a glioblastoma validation cohort compared to ExAC controls (0.00193 and 0.00298, respectively). In addition, three novel and one rare *ADAR* variants not previously associated with AGS were identified in the glioblastoma test and validation cohorts (Supplementary Tables 9, 10). The variants *ADAR,*c.577C>G;p.(P193A) and *RNASEH2B,*c.529G>A;p.(A177T), detected in one glioblastoma each, were also found in non-neoplastic tissue of the same patients (patient II.1 of family 3 and family 4), indicating that they were in fact germline alterations (Fig. 1c, d; Supplementary Fig. 1c, d). Furthermore, in addition to the *RNASEH2B,*c.529G>A;p.(A177T) variant in the glioblastoma of patient II.1 of family 4, the novel *ADAR* variant c.2891C>T;p.(A964V) was found, demonstrating that the tumor was simultaneously heterozygous for *ADAR* and *RNASEH2B* variants (Supplementary Table 10). Finally, we performed targeted sequencing of *ADAR* and *RNASEH2B* hot spot exons (see Materials and methods) in a test (n=15) and a validation cohort (n=50) of prostate carcinomas, to determine if our findings in glioblastoma also apply to prostate carcinoma. The allele frequency for *ADAR,*c.577C>G;p.(P193A) was 11 times higher in the prostate carcinoma test cohort (0.03333; 1 in 30 alleles) compared to ExAC controls (0.00298), whereas *RNASEH2B,*c.529G>A;p.(A177T) was 17 times higher in the test (0.03333; 1 in 30 alleles) and 5 times higher in the validation (0.01000; 1 in 100 alleles) cohort compared to ExAC controls (0.00193). In addition, the novel *RNASEH2B* variant c.608A>G;p.(D203G) was detected in one patient in the validation cohort (Supplementary Tables 9, 10). Again, the AGS-associated variants *ADAR,*c.577C>G;p.(P193A) and *RNASEH2B,*c.529G>A;p.(A177T) were germline alterations as indicated by their presence in DNA from non-neoplastic lymph node from the same patients (Fig. 1e; Supplementary Fig. 1e; Fig. 1f; Supplementary Fig. 1f). All gliomas harboring *ADAR* and/or *RNASEH2B* variants had no co-deletion of chromosomal arms 1p and 19q (Supplementary Table 10), and were thus of astrocytic origin according to the current WHO classification of tumors of the central nervous system [40].

In summary, we detect novel variants and increased allele frequencies of certain rare variants in the AGS-associated genes *ADAR* and *RNASEH2B* in the germline and tumors of glioma and prostate carcinoma patients, suggesting an association of *ADAR* and *RNASEH2B*

alterations with glioma and prostate carcinoma risk and tumorigenesis, whereby germline variants in other genes may additionally contribute to tumor risk in these patients.

The *ADAR* p.(P193A) variant destabilizes the protein-Z-DNA complex resulting in a partial unbinding of the Z-DNA, and affects tumor cell proliferation

To gain insights into the effect of the ADAR p.(P193A) variant detected in the germline of glioma and prostate carcinoma patients at the molecular level, molecular dynamics simulations were carried out. Proline 193 is located in the Z-DNA/Z-RNA binding domain (designated Zα) of ADAR, and is part of a β-hairpin motif (β-wing) directly involved in Z-DNA interaction. P193 mainly contributes to Z-DNA binding through hydrophobic interactions [64]. Therefore by using molecular dynamics simulations, a comparison of the structure and conformational dynamics of the Zα domain in wildtype and mutant ADAR together with the bound Z-DNA could be made. As compared to wildtype ADAR, the p.(P193A) variant significantly increased the flexibility of the protein, leading to large structural fluctuation, in particular of Z-DNA binding elements, including helices α2 and α3, as well as the β-wing (β2 to β3) (Fig. 2a, b). Along the molecular dynamics simulation, these fluctuations disturbed the well-defined Z-DNA binding area and impaired shape complementarity resulting in an unbinding of the 3' end of the Z-DNA and large conformational changes, thereby destabilizing the protein-Z-DNA complex (Fig. 2c, d). Next, we aimed to determine whether the *ADAR* p.(P193A) variant might facilitate tumorigenesis by affecting proliferation. Human LN-229 glioma and human HCT116 colorectal cancer cells stably expressing either wildtype interferon-induced ADAR p150 protein or the ADAR p.(P193A) variant were generated (Supplementary Fig. 3a), and growth kinetics were determined. While expression of wildtype ADAR caused a reduced proliferation of tumor cells as compared to vector control, expression of the ADAR p.(P193A) variant did not result in this growth suppressive effect (Supplementary Fig. 3b-g). Our findings provide *in silico* and *in vitro* evidence that the ADAR p.(P193A) variant may play a role in tumorigenesis by impairing Z-DNA interaction and enhancing cell proliferation.

Detected rare *RNASEH2B* variants cause increased double-strand DNA damage and impair ribonucleotide excision repair

The RNase H2 complex is critical for the removal of ribonucleotides misincorporated into genomic DNA during replication and repair, and for the maintenance of genome integrity. MEFs from *Rnaseh2b*$^{-/-}$ mice display widespread genome instability, with γH2AX, a marker of DNA-damage response to double-strand breaks, substantially increased [56]. We explored the ability of wildtype versus mutant Rnaseh2b to rescue this DNA damage phenotype. Expression of the mutant murine proteins corresponding to the rare variants detected in glioma and prostate carcinoma patients, p.(K162N) and p.(A174T), in *Rnaseh2b*$^{-/-}$ MEFs (Supplementary Fig. 4) showed significantly reduced rescue from DNA damage compared to wildtype Rnaseh2b (Fig. 3a). Comparable results were obtained in patient-derived human fibroblasts (Fig. 3b). In comparison to fibroblasts from four controls, cells from patient II.2 of family 2, carrying the *RNASEH2B,*c.529G>A;p.(A177T) alteration, were characterized by a significantly higher number of nuclear γH2AX foci (Fig. 3b). The observed DNA damage in RNase H2 deficient cells is generally thought to be the result of the impaired removal of misincorporated ribonucleotides. Consistent with this, we found that after expression of the Rnaseh2b p.(K162N) and p.(A174T) variants in *Rnaseh2b*$^{-/-}$ MEFs, isolated genomic DNA was more sensitive to RNase HII digestion as compared to *Rnaseh2b*$^{-/-}$ MEFs rescued with wildtype Rnaseh2b (Fig. 3c, d). This finding reflects a higher ribonucleotide content in the genomic DNA of *Rnaseh2b*$^{-/-}$ MEFs transfected with Rnaseh2b mutants versus wildtype Rnaseh2b. Our results suggest that the *RNASEH2B* germline variants identified in glioma and prostate carcinoma patients may promote tumorigenesis through increased double-strand DNA damage resulting from defective removal of genome-embedded ribonucleotides.

Patients with rare *ADAR* or *RNASEH2B* mutations and their tumors recapitulate features of the AGS type I interferonopathy

Cerebral atrophy and leukoencephalopathy were described in over 90% of children with AGS and commonly showed frontotemporal predominance [38]. Therefore, we evaluated tumor localization

and neuroradiological findings in glioma patients carrying rare *ADAR* or *RNASEH2B* germline variants. All four gliomas were located in the frontal or temporal lobe (Supplementary Table 10), and one of four patients showed bifrontal lobe atrophy (Fig. 4a). Brain calcification is another classical hallmark of AGS [2, 38]. Therefore, we assessed the presence of calcifications in gliomas or non-neoplastic brain of patients carrying rare *ADAR* or *RNASEH2B* variants. Calcifications were detected in the tumor or non-neoplastic brain of all four glioma patients with *ADAR* or *RNASEH2B* germline variants analyzed histologically, whereby these were numerous or large in two of the four cases (Supplementary Tables 10, 11; Fig. 4b, c; Supplementary Fig. 5a, b). Compared to five gliomas without *ADAR* or *RNASEH2B* variants, the six gliomas with *ADAR* or *RNASEH2B* variants showed an increased calcification score (Fig. 4d). Calcifications were also significantly more frequent in prostate carcinomas with versus without *ADAR* or *RNASEH2B* variants (Supplementary Fig. 5c-e; Supplementary Table 11).

To test whether type I IFNs are upregulated in *ADAR* or *RNASEH2B* variant-positive gliomas comparable to the findings in the CSF of AGS patients [62, 63], we determined the protein expression of interferon alpha 6 (IFNA6) by immunostaining of glioma sections. We observed that gliomas with *ADAR* or *RNASEH2B* variants showed a significantly higher IFNA6 expression in the cytoplasm of glial cells as compared to gliomas without *ADAR* or *RNASEH2B* variants (Fig. 4e-h; Supplementary Fig. 6; Supplementary Table 11). Previously, it was reported that the type I IFN-inducible chemokine CXCL10 was elevated in the CSF and plasma of AGS patients [57, 62, 63], and in skin lesions from patients with systemic lupus erythematosus (SLE) carrying heterozygous *RNASEH2B* variants [23]. Therefore, we performed CXCL10 immunostaining on tissue sections from gliomas with and without *ADAR* or *RNASEH2B* variants. Whereas *ADAR* or *RNASEH2B* variant-negative gliomas had a low mean CXCL10 score, gliomas with *ADAR* or *RNASEH2B* variants showed significantly enhanced CXCL10 expression in glial cells (Fig. 4i-l; Supplementary Fig. 6; Supplementary Table 11). Increased IFNA6 and CXCL10 expression was paralleled by a significantly higher CD68 expression in gliomas with versus without *ADAR* or *RNASEH2B* variants, consistent with an enhanced, IFNA6/CXCL10-induced recruitment of

macrophages and microglial cells into *ADAR* or *RNASEH2B* variant-positive tumors (Supplementary Fig. 7; Supplementary Table 11).

AGS has also been associated with increased expression of ISG transcripts in peripheral blood [15, 60]. Therefore, we assessed the expression of six genes significantly upregulated in AGS patients with biallelic *ADAR* mutations, i.e. *IFI27*, *IFI44L*, *IFIT1*, *ISG15*, *RSAD2*, *SIGLEC1* [60], in whole blood from three glioma patients carrying AGS-associated *ADAR* or *RNASEH2B* germline mutations. Transcript levels of *IFI27*, *IFIT1*, and *RSAD2* were significantly increased in peripheral blood of these glioma patients as compared to twenty controls matching the patients in gender and age, while *IFI44L*, *ISG15*, and *SIGLEC1* mRNA levels did not differ in glioma patients and controls (Fig. 4m; Supplementary Fig. 8).

Our findings indicate that the detected germline or somatic variants in both *ADAR* and *RNASEH2B* are associated with features of the AGS type I interferonopathy in glioma and prostate carcinoma tissue as well as in patients affected by these tumors. More specifically, our results provide *in vivo* evidence that these variants lead to upregulation of IFN as well as IFN-induced genes, and suggest that they may contribute to tumorigenesis via enhanced interferon type I signaling.

Enhanced ISG expression *in vitro* due to rare *ADAR* and *RNASEH2B* variants can be blocked by janus kinase (JAK) 1/2 inhibitor Ruxolitinib

To confirm that the increase of ISG transcripts detected in the peripheral blood of glioma patients is due to *ADAR* and *RNASEH2B* variants, LN-229 cells were transiently transfected with wildtype or mutant *ADAR* or *RNASEH2B* constructs (Supplementary Fig. 9), and *IFI27*, *IFIT1*, and *RSAD2* mRNA levels were quantified. Expression of *IFI27*, *IFIT1*, and *RSAD2* was significantly higher in tumor cells expressing ADAR p.(P193A) as well as RNASEH2B p.(K165N) and RNASEH2B p.(A177T) mutants as compared to wildtype ADAR or RNASEH2B, indicating an IFN type I response (Fig. 5a).

With the aim to identify therapeutic or prophylactic compounds for individuals carrying pathogenic *ADAR* or *RNASEH2B* variants, we used this cellular model to study signaling

pathways involved in ADAR and RNASEH2B mediated induction of ISG expression. It has been proposed that ADAR inactivation induces a type I IFN response and enhanced ISG expression via phosphorylation and subsequent nuclear translocation of transcription factor IRF3 [49]. Therefore, we compared nuclear IRF3 accumulation indicative of pIRF3 levels between LN-229 cells expressing wildtype or mutant ADAR or RNASEH2B. Immunofluorescence revealed that a significantly higher percentage of cells had an elevated nuclear IRF3 score indicating increased levels of transcriptionally active IRF3 upon transient expression of mutant compared to wildtype ADAR and RNASEH2B (Fig. 5b, c; Supplementary Fig. 10). Our results suggest that the elevated ISG expression seen with mutant ADAR and RNASEH2B involves activation and nuclear translocation of IRF3.

Recently, constitutive epidermal growth factor receptor (EGFR) signaling was shown to activate IRF3 leading to increased expression of *IFI27* and *IFIT1* via the JAK/STAT1/2 pathway, which could be blocked by the JAK inhibitor Ruxolitinib in glioblastoma cell lines [10]. Therefore, we explored whether Ruxolitinib would have the same effect on high ISG expression induced by mutant ADAR or RNASEH2B in glioblastoma cells, in which we had shown IRF3 activation. We incubated LN-229 cells expressing wildtype or mutant ADAR or RNASEH2B with Ruxolitinib and expression of *IFI27*, *IFIT1*, and *RSAD2* was quantified. Ruxolitinib treatment was found to abrogate the elevated ISG transcription levels seen for mutant ADAR and RNASEH2B (Fig. 5d). In summary, glioblastoma cells expressing mutant ADAR or RNASEH2B show a type I IFN response via activation of IRF3 that can be blocked by the JAK inhibitor Ruxolitinib, indicating that JAK/STAT signaling is involved. Our results suggest that glioma patients carrying germline mutations in *ADAR* or *RNASEH2B* might benefit from JAK inhibitors such as Ruxolitinib for the treatment of a glioma or prostate carcinoma or as an agent for tumor prevention.

Discussion

Here, we provide data suggesting that rare *ADAR* and *RNASEH2B* variants are associated with glioma and prostate carcinoma risk and tumorigenesis as well as a type I interferon signature.

The starting point of this study was family 1 with a clinically presumed susceptibility for glioma and prostate carcinoma because of four affected individuals in three consecutive generations. By whole-exome sequencing, three family members affected by *IDH1*-mutant anaplastic gliomas or prostate carcinoma were found to be simultaneously heterozygous for rare germline variants in *ADAR* and *RNASEH2B*, while three unaffected family members were not. Previously, homozygous or compound heterozygous mutations of *ADAR* and *RNASEH2B* have been reported to cause AGS [17, 60], whereby the *ADAR* c.577C>G;p.(P193A) variant detected here in German cancer family 1 and found to be enriched 3- to 11-fold in the germline and tumor DNA of glioblastoma and prostate carcinoma test and/or validation cohorts as compared to ExAC controls, was described in five AGS families of European ancestry [60]. This alteration lies in the Zα domain of the adenosine deaminase, which specifically recognizes DNA and RNA in a higher energy Z-conformation, and only affects the IFN-inducible p150 isoform of ADAR. Here, molecular dynamics simulations indicate an increased structural flexibility of the ADAR Zα domain due to the p.(P193A) variant, which significantly affected the Z-DNA/Z-RNA binding area, impairing Z-DNA interaction and destabilizing the protein-Z-DNA complex. Our findings are consistent with previous results that binding of Z-DNA to the ADAR Zα domain is shape-specific [24, 29, 64]. Moreover, our simulations may have identified the structural basis underlying both the altered RNA editing activity described previously [44] and the impaired growth suppression of the ADAR p.(P193A) variant shown here, as compared to the growth suppressive effect of wildtype ADAR reported here and previously [50]. Both effects may be linked since changes of RNA editing levels may be a general mechanism to promote tumor growth [66]. Furthermore, localization of the ADAR p.(P193A) variant to cytoplasmic stress granules, which requires a functional Zα domain [47], may be impaired.

In addition to the novel *RNASEH2B* variant in family 1, we detected the *RNASEH2B* c.529G>A;p.(A177T) alteration, previously reported in 14 of 18 AGS families of European or North-African descent [17], in the glioblastoma patient of German cancer family 2 resulting in a significantly higher frequency of rare deleterious *RNASEH2B* variants in the germline of familial glioma patients than in ExAC controls. As shown in *Rnaseh2b*$^{-/-}$ MEFs, both *Rnaseh2b* variants

impact on ribonucleotide excision repair and DNA damage. Additionally, fibroblasts from our glioblastoma patient carrying the *RNASEH2B* c.529G>A;p.(A177T) alteration showed signs of chronic low-level DNA damage, as described previously for fibroblasts with a heterozygous *RNASEH2B* mutation from an SLE patient [23]. That report demonstrates a significant contribution of rare variants of the *RNASEH2* genes, *RNASEH2A, RNASEH2B,* and *RNASEH2C,* to SLE risk [23]. Taken together, the study by Günther et al. and our report extend the phenotypic spectrum caused by *ADAR* and *RNASEH2B* genetic variation beyond AGS to SLE and glioma and prostate carcinoma risk. This link is not unexpected because SLE patients have an overall increased risk of malignancy compared with the general population [22]. A direct association between AGS genes and other cancer types was suggested by two recent studies [14, 51]. Clifford and colleagues reported on a homozygous germline *SAMHD1* mutation in an AGS patient who developed CLL at 24 years of age, and acquired *SAMHD1* mutations in around 10% of relapsed/refractory CLL patients [14]. Studying over 10,000 cases and over 20,000 controls, Permuth and colleagues found a significant association between genetic variation in *ADAR* and epithelial ovarian cancer susceptibility [51].

Our study provides evidence that rare variants in both AGS genes found altered here, *ADAR* and *RNASEH2B,* are associated with features of the AGS type I interferonopathy in tumors and tumor patients, whereby the patients were not affected by the full spectrum of AGS symptoms because they were heterozygous or simultaneously heterozygous mutation carriers. First, seven of eight gliomas with an *ADAR* or *RNASEH2B* variant were located in the frontotemporal brain, where AGS associated leukoencephalopathy is predominant [38]. Second, calcification, an AGS hallmark usually occurring in the brain [2, 38], was more likely in gliomas and significantly more pronounced in prostate carcinomas with *ADAR* or *RNASEH2B* variants than without. Third, expression of IFNA and of type I IFN-inducible CXCL10, produced by astrocytes in AGS [63], was elevated in gliomas with *ADAR* and *RNASEH2B* variants compared to *ADAR* and *RNASEH2B* wildtype gliomas. Similarly, high CXCL10 expression was previously observed in lesional skin from an SLE patient carrying a heterozygous *RNASEH2B* variant [23]. Fourth, similar to AGS patients and their heterozygous parents [15, 60], increased expression of a subset of ISG

transcripts (*IFI27*, *IFIT1* and *RSAD2*) was found in peripheral blood of glioma patients carrying germline *ADAR* and/or *RNASEH2B* variants.

The link between *ADAR* and *RNASEH2B* variants and enhanced expression of certain ISGs was corroborated by our finding that elevated levels of *IFI27*, *IFIT1* and *RSAD2* could also be induced *in vitro* by expressing *ADAR* and *RNASEH2B* variants in tumor cells. Using this cellular model, we found that stimulation of ISG expression by *ADAR* and *RNASEH2B* variants is mediated by activation of the transcription factor IRF3, known to play a key role in antiviral innate immunity. It was recently shown that IRF3 is also activated by constitutive EGFR signaling leading to expression of *IFI27* and *IFIT1* in glioblastomas [10]. Aberrant EGFR signaling caused by EGFR amplification and/or constitutively activating mutation is common in human tumors including malignant astrocytic gliomas and prostate carcinomas [3, 11], and enhances tumorigenicity [33]. Here, we propose that germline or somatic *ADAR* and *RNASEH2B* variants result in the same downstream signals as constitutively active EGFR, thus representing an alternative mechanism for tumorigenesis in certain cancers such as gliomas and prostate carcinomas, whereby tumor initiation is enhanced by *ADAR* and *RNASEH2B* germline variants as opposed to malignant progression by somatic deregulation of EGFR signaling. IFN pathway activation by constitutive EGFR signaling via IRF3 was abolished by JAK inhibitor Ruxolitinib [10], as might be expected because IRF3 activates the JAK-STAT pathway by stimulating IFN-β transcription leading to the transcription of ISGs. Here, we show that Ruxolitinib also suppresses *ADAR* and *RNASEH2B* variant-mediated expression of the ISGs *IFI27* and *IFIT1*. Thus, targeting the JAK-STAT pathway by inhibitors may have prophylactic or therapeutic potential in individuals carrying pathogenic *ADAR* and *RNASEH2B* variants regarding the tumor phenotype. Previous studies have indicated that the JAK2 inhibitor AZD1480 suppresses the growth of human xenografts from prostate cancer cells [28], and from glioma cells thus increasing the survival of mice bearing intracranial glioblastoma xenografts [45], supporting the development of JAK inhibitors for the treatment and possibly the prevention of solid tumors in individuals with *ADAR* and *RNASEH2B* variants.

We propose that rare *ADAR* and *RNASEH2B* germline variants specifically increase the risk for diffusely infiltrating gliomas without co-deletion of chromosomal arms 1p and 19q, which may, however, carry *IDH1* mutations or not. According to the current WHO classification of tumors of the central nervous system, diffuse gliomas without 1p/19q deletion are astrocytic tumors [40]. Furthermore, the *IDH* mutation status is a major classification parameter for gliomas [40]. Our data suggest that in the brain, rare *ADAR* and *RNASEH2B* germline variants lead to astrocytic tumors only, which may then acquire *IDH1* mutations or not. From a transgenic mouse with CNS expression of IFNA, we know that the neuropathologic changes include astrocyte hypertrophy, progressive calcification, and up-regulation of a number of IFNA-regulated genes [8], mimicking the findings in the diffuse astrocytic tumors with rare *ADAR* and *RNASEH2B* variants described here. Therefore, the type I interferonopathy in patients carrying rare *ADAR* and *RNASEH2B* germline variants may specifically impact astrocytes or astroglial progenitors in the brain, thereby increasing the risk for the development of astrocytic gliomas. Recently, astrocytes were shown to produce IFNA as a paracrine signal that supports metastatic tumor growth, providing evidence for an association between inflammatory cytokines, such as IFNA, and growth of brain metastatic cells [12]. Mediated by dsDNA, metastatic cancer cells triggered astrocyte cytokine release via cGAS by transferring cGAMP through gap junctions into neighboring astrocytes, where IRF3 was activated via STING [12]. A role for the IFN stimulator STING in the control of cancer was shown in *STING*$^{-/-}$ mice, which were largely resistant to skin carcinogenesis induced by a mutagen causing accumulation of nuclear DNA in the cytosol, a trigger leading to intrinsic cytokine production and tumor development in a *STING* wildtype setting [1]. The cGAS/STING nucleic acid-sensing pathway is also relevant to AGS as reported in the *Rnaseh2b*$^{G37S/G37S}$ and the *Rnaseh2b*$^{A174T/A174T}$ knock-in mice [42, 53]. Therefore, data from this and other studies provide direct and indirect evidence for an association between AGS-related gene mutations and type I IFN-induced tumorigenesis, whereas the study of cancer risk in patients with AGS is hampered by the fact that the severe neurological dysfunction often causes lethality in childhood, with only around 2% of patients still alive at more than 30 years of age [15].

IDH1 is another gene, in which an association between somatic mutation, inflammation, and glioma tumorigenesis is proposed, whereby the starting point is the formation of the oncometabolite 2-hydroxyglutarate leading to over-excitation of NMDA receptors, increased IL-1β production, and IL-6 induction via the JAK/STAT pathway [46]. In the gliomas with somatic *IDH1* mutations of our study, the germline *ADAR* and/or *RNASEH2B* variants will have preceded this mutation, while in the tumor cells variation in all three genes may additively promote inflammation and drive tumor progression. However, since *IDH1* mutations were not detected in most gliomas with *ADAR* and/or *RNASEH2B* variants described here, *ADAR* and *RNASEH2B* variants may represent genetic equivalents of *IDH1* mutations in inducing inflammation-driven malignant transformation.

In summary, our results link *ADAR* and *RNASEH2B*, previously associated with the inflammatory disease AGS and the autoimmune disorder SLE, and an enhanced type I IFN response to glioma and prostate carcinoma risk and tumorigenesis. Furthermore, we propose that targeting the type I IFN signaling axis by inhibitors may have prophylactic or therapeutic potential regarding a tumor phenotype in individuals carrying pathogenic *ADAR* and *RNASEH2B* variants.

Acknowledgements The authors wish to thank the patients and their families for participating in this study, and all colleagues, patients and families supporting the German Glioma Network. We acknowledge Andrew P. Jackson, Edinburgh, U.K. for helpful discussions, Vanessa Dewor and Wiebke Schulze, Hannover, Germany for excellent technical assistance, and Alma Osmanovic, Hannover, Germany for performing the skin biopsy on patient II.2 of family 2. pCMV-HA-ADAR wildtype constructs and the pIRESneo vector were kindly provided by Yanick Crow, Manchester, U.K. and Paris, France, and Matthias Dobbelstein, Göttingen, Germany, respectively.

Authors contributions UB, FB, MAMR, MP, and RGW designed research; UB, FB, HM, JW, AC, NE, AE, MP, and CH performed research; BH, MaW, GS, TP, BH, JKK, AS, PR, AD, CAD, IES, OWH, AE, UL, GR, MiW, MAMR, BW, and CH contributed materials, patient/tumor data and expertise; UB, FB, JW, MP, and RGW analyzed data and made figures; UB, FB, MAMR, MP, and RGW wrote the manuscript; all authors reviewed and revised the manuscript.

Compliance with ethical standards

Statement of human rights The study was approved by the appropriate institutional research ethics committees. All procedures were in accordance with their ethical standards and with the 1964 Helsinki declaration and its later amendments or comparable ethical standards.

Funding This work was supported by the German Cancer Aid (Deutsche Krebshilfe e.V.; Grant No. 70-3163-Wi 3).

Conflict of Interest GR has received research grants from Roche and Merck (EMD, Darmstadt), as well as honoraria for lectures or advisory boards from Amgen, Celldex and Medac. JKK is a consultant to Medtronic and Boston Scientific, and received fees for speaking from St. Jude Medical Inc. / AbbVie. All other authors declare that they have no conflict of interest.

References

1. Ahn J, Xia T, Konno H, Konno K, Ruiz P, Barber GN (2014) Inflammation-driven carcinogenesis is mediated through STING. Nat Commun 5:5166
2. Aicardi J, Goutières F (1984) A progressive familial encephalopathy in infancy with calcifications of the basal ganglia and chronic cerebrospinal fluid lymphocytosis. Ann Neurol 15:49-54
3. Aldape K, Zadeh G, Mansouri S, Reifenberger G, von Deimling A (2015) Glioblastoma: pathology, molecular mechanisms and markers. Acta Neuropathol 129:829-848
4. Al Olama AA, Kote-Jarai Z, Giles GG, Guy M, Morrison J, Severi G et al (2009) Multiple loci on 8q24 associated with prostate cancer susceptibility. Nat Genet 41:1058-1060
5. Bainbridge MN, Armstrong GN, Gramatges MM, Bertuch AA, Jhangiani SN, Doddapaneni H, et al (2014) Germline mutations in shelterin complex genes are associated with familial glioma. J Natl Cancer Inst 107:384
6. Benjamini Y, Hochberg Y (1995) Controlling the false discovery rate: a practical and powerful approach to multiple testing. J R Statist Soc B 57:289-300
7. Best RB, Zhu X, Shim J, Lopes PE, Mittal J, Feig M et al (2012) Optimization of the additive CHARMM all-atom protein force field targeting improved sampling of the backbone φ, ψ and side-chain χ(1) and χ(2) dihedral angles. J Chem Theory Comput 8:3257-3273
8. Campbell IL, Krucker T, Steffensen S, Akwa Y, Powell HC, Lane T et al (1999) Structural and functional neuropathology in transgenic mice with CNS expression of IFN-alpha. Brain Res 835:46-61
9. Capper D, Weissert S, Balss J, Habel A, Meyer J, Jäger D et al (2010) Characterization of R132H mutation-specific IDH1 antibody binding in brain tumors. Brain Pathol 20:245-254
10. Chakraborty S, Li L, Puliyappadamba VT, Guo G, Hatanpaa KJ, Mickey B et al (2014) Constitutive and ligand-induced EGFR signalling triggers distinct and mutually exclusive downstream signalling networks. Nat Commun 5:5811
11. Chappell WH, Abrams SL, Lertpiriyapong K, Fitzgerald TL, Martelli AM, Cocco L et al (2016) Novel roles of androgen receptor, epidermal growth factor receptor, TP53, regulatory RNAs, NF-kappa-B, chromosomal translocations, neutrophil associated gelatinase, and matrix metalloproteinase-9 in prostate cancer and prostate cancer stem cells. Adv Biol Regul 60:64-87
12. Chen Q, Boire A, Jin X, Valiente M, Er EE, Lopez-Soto A et al (2016) Carcinoma-astrocyte gap junctions promote brain metastasis by cGAMP transfer. Nature 20533:493-498
13. Classen CF, Riehmer V, Landwehr C, Kosfeld A, Heilmann S, Scholz C et al (2013) Dissecting the genotype in syndromic intellectual disability using whole exome sequencing in addition to genome-wide copy number analysis. Hum Genet 132:825-841
14. Clifford R, Louis T, Robbe P, Ackroyd S, Burns A, Timbs AT et al (2014) SAMHD1 is mutated recurrently in chronic lymphocytic leukemia and is involved in response to DNA damage. Blood 123:1021-1031
15. Crow YJ, Chase DS, Lowenstein Schmidt J, Szynkiewicz M, Forte GM, Gornall HL et al (2015) Characterization of human disease phenotypes associated with mutations in TREX1, RNASEH2A, RNASEH2B, RNASEH2C, SAMHD1, ADAR, and IFIH1. Am J Med Genet A 167A:296-312

16. Crow YJ, Hayward BE, Parmar R, Robins P, Leitch A, Ali M et al (2006) Mutations in the gene encoding the 3'-5' DNA exonuclease TREX1 cause Aicardi-Goutières syndrome at the AGS1 locus. Nat Genet 38:917-920
17. Crow YJ, Leitch A, Hayward BE, Garner A, Parmar R, Griffith E et al (2006) Mutations in genes encoding ribonuclease H2 subunits cause Aicardi-Goutières syndrome and mimic congenital viral brain infection. Nat Genet 38:910-916
18. Crow YJ, Manel N (2015) Aicardi-Goutières syndrome and the type I interferonopathies. Nature Rev Immunol 15:429-440
19. Darden T, York D, Pedersen L (1993) Particle mesh Ewald: An *N* • log(*N*) method for Ewald sums in large systems. J Chem Phys 98:10089-10092
20. Felsberg J, Rapp M, Loeser S, Fimmers R, Stummer W, Goeppert M et al (2009) Prognostic significance of molecular markers and extent of resection in primary glioblastoma patients. Clin Cancer Res 15:6683-6693
21. Felsberg J, Wolter M, Seul H, Friedensdorf B, Göppert M, Sabel MC et al (2010) Rapid and sensitive assessment of the IDH1 and IDH2 mutation status in cerebral gliomas based on DNA pyrosequencing. Acta Neuropathol 119:501-507
22. Goobie GC, Bernatsky S, Ramsey-Goldman R, Clarke AE (2015) Malignancies in systemic lupus erythematosus: a 2015 update. Curr Opin Rheumatol 27:454-460
23. Günther C, Kind B, Reijns MA, Berndt N, Martinez-Bueno M, Wolf C et al (2015) Defective removal of ribonucleotides from DNA promotes systemic autoimmunity. J Clin Invest 125:413-424
24. Ha SC, Choi J, Hwang HY, Rich A, Kim YG, Kim KK (2009) The structures of non-CG-repeat Z-DNAs co-crystallized with the Z-DNA-binding domain, hZ alpha(ADAR1). Nucleic Acids Res 37:629-637
25. Hart K, Foloppe N, Baker CM, Denning EJ, Nilsson L, Mackerell AD Jr (2012) Optimization of the CHARMM additive force field for DNA: Improved treatment of the BI/BII conformational equilibrium. J Chem Theory Comput 8:348-362
26. Hartmann C, Meyer J, Balss J, Capper D, Mueller W, Christians A et al (2009) Type and frequency of IDH1 and IDH2 mutations are related to astrocytic and oligodendroglial differentiation and age: a study of 1,010 diffuse gliomas. Acta Neuropathol 118:469-474
27. Hartner JC, Walkley CR, Lu J, Orkin SH (2009) ADAR1 is essential for the maintenance of hematopoiesis and suppression of interferon signaling. Nat Immunol 10:109-115
28. Hedvat M, Huszar D, Herrmann A, Gozgit JM, Schroeder A, Sheehy A et al (2009) The JAK2 inhibitor AZD1480 potently blocks Stat3 signaling and oncogenesis in solid tumors. Cancer Cell 16:487-497
29. Herbert A, Schade M, Lowenhaupt K, Alfken J, Schwartz T, Shlyakhtenko LS et al (1998) The Zalpha domain from human ADAR1 binds to the Z-DNA conformer of many different sequences. Nucleic Acids Res 26:3486-3493
30. Hiller B, Achleitner M, Glage S, Naumann R, Behrendt R, Roers A (2012) Mammalian RNase H2 removes ribonucleotides from DNA to maintain genome integrity. J Exp Med 209:1419-1426
31. Hofer MJ, Campbell IL (2013) Type I interferon in neurological disease-the devil from within. Cytokine Growth Factor Rev 24:257-267
32. Hogg M, Paro S, Keegan LP, O'Connell MA (2011) RNA editing by mammalian ADARs. Adv Genet 73:87-120
33. Huang HS, Nagane M, Klingbeil CK, Lin H, Nishikawa R, Ji XD et al (1997) The enhanced

tumorigenic activity of a mutant epidermal growth factor receptor common in human cancers is mediated by threshold levels of constitutive tyrosine phosphorylation and unattenuated signaling. J Biol Chem 272:2927-2935

34. Hwang T, Park CK, Leung AK, Gao Y, Hyde TM, Kleinman JE et al (2016) Dynamic regulation of RNA editing in human brain development and disease. Nat Neurosci 19:1093-1099
35. Jenkins RB, Xiao Y, Sicotte H, Decker PA, Kollmeyer TM, Hansen HM et al (2012) A low-frequency variant at 8q24.21 is strongly associated with risk of oligodendroglial tumors and astrocytomas with IDH1 or IDH2 mutation. Nat Genet 44:1122-1125
36. Johansson G, Andersson U, Melin B (2016) Recent developments in brain tumor predisposing syndromes. Acta Oncol 55:401-411
37. Jorgensen WL, Chandrasekhar J, Madura JD, Impey RW, Klein ML (1983) Comparison of simple potential functions for simulating liquid water. J Chem Phys 79:926-935
38. La Piana R, Uggetti C, Roncarolo F, Vanderver A, Olivieri I, Tonduti D et al (2016) Neuroradiologic patterns and novel imaging findings in Aicardi-Goutières syndrome. Neurology 86:28-35
39. Lek M, Karczewski KJ, Minikel EV, Samocha KE, Banks E, Fennell T et al (2016) Analysis of protein-coding genetic variation in 60,706 humans. Nature 536:285-291
40. Louis DN, von Deimling A, Cavenee WK (2016) Diffuse astrocytic and oligodendroglial tumours – Introduction. In: Louis DN, Ohgaki H, Wiestler OD, Cavenee WK (eds) WHO Classification of Tumours of the Central Nervous System (revised 4th edition). International Agency for Research on Cancer, Lyon, pp 16-17
41. Lynch HT, Kosoko-Lasaki O, Leslie SW, Rendell M, Shaw T, Snyder C et al (2016) Screening for familial and hereditary prostate cancer. Int J Cancer 138:2579-2591
42. Mackenzie KJ, Carroll P, Lettice L, Tamauskaite Z, Reddy K, Dix F et al (2016) Ribonuclease H2 mutations induce a cGAS/STING dependent innate immune response. Embo J 35:831-844
43. Malmer B, Grönberg H, Bergenheim AT, Lenner P, Henriksson R (1999) Familial aggregation of astrocytoma in northern Sweden: an epidemiological cohort study. Int J Cancer 81:366-370
44. Mannion NM, Greenwood SM, Young R, Cox S, Brindle J, Read D et al (2014) The RNA-editing enzyme ADAR1 controls innate immune responses to RNA. Cell Rep 9:1482-1494
45. McFarland BC, Ma JY, Langford CP, Gillespie GY, Yu H, Zheng Y et al (2011) Therapeutic potential of AZD1480 for the treatment of human glioblastoma. Mol Cancer Ther 10:2384-2393
46. Michelson N, Rincon-Torroella J, Quiñones-Hinojosa A, Greenfield JP (2016) Exploring the role of inflammation in the malignant transformation of low-grade gliomas. J Neuroimmunol 297:132-140
47. Ng SK, Weissbach R, Ronson GE, Scadden AD (2013) Proteins that contain a functional Z-DNA-binding domain localize to cytoplasmic stress granules. Nucleic Acids Res 41:9786-9799
48. Nick McElhinny SA, Watts, BE, Kumar D, Watt DL, Lundström EB, Burgers PM et al (2010) Abundant ribonucleotide incorporation into DNA by yeast replicative polymerases. Proc Natl Acad Sci USA 107:4949-4954
49. O'Connell MA, Mannion NM, Keegan LP (2015) The Epitranscriptome and Innate Immunity. PLoS Genet 11:e1005687

50. Paz N, Levanon EY, Amariglio N, Heimberger AB, Ram Z, Constantini S et al (2007) Altered adenosine-to-inosine RNA editing in human cancer. Genome Res 17:1586-1595
51. Permuth JB, Reid B, Earp M, Chen YA, Monteiro AN, Chen Z et al (2016) Inherited variants affecting RNA editing may contribute to ovarian cancer susceptibility: results from a large-scale collaboration. Oncotarget 7:72381-72394
52. Phillips JC, Braun R, Wang W, Gumbart J, Tajkhorshid E, Villa E et al (2005) Scalable molecular dynamics with NAMD. J Comput Chem 26:1781-1802
53. Pokatayev V, Hasin N, Chon H, Cerritelli SM, Sakhuja K, Ward JM et al (2016) RNase H2 catalytic core Aicardi-Goutières syndrome-related mutant invokes cGAS-STING innate immune-sensing pathway in mice. J Exp Med 213:329-336
54. Reifenberger G, Weber RG, Riehmer V, Kaulich K, Willscher E, Wirth H et al (2014) Molecular characterization of long-term survivors of glioblastoma using genome- and transcriptome-wide profiling. Int J Cancer 135:1822-1831
55. Reijns MA, Jackson AP (2014) Ribonuclease H2 in health and disease. Biochem Soc Trans 42:717-725
56. Reijns MA, Rabe B, Rigby RE, Mill P, Astell KR, Lettice LA et al (2012) Enzymatic removal of ribonucleotides from DNA is essential for mammalian genome integrity and development. Cell 149:1008-1022
57. Rice G, Patrick T, Parmar R, Taylor CF, Aeby A, Aicardi J et al (2007) Clinical and molecular phenotype of Aicardi-Goutieres syndrome. Am J Hum Genet 81:713-725
58. Rice GI, Bond J, Asipu A, Brunette RL, Manfield IW, Carr IM et al (2009) Mutations involved in Aicardi-Goutières syndrome implicate SAMHD1 as regulator of the innate immune response. Nat Genet 41:829-832
59. Rice GI, del Toro Duany Y, Jenkinson EM, Forte GM, Anderson BH, Ariaudo G et al (2014) Gain-of-function mutations in IFIH1 cause a spectrum of human disease phenotypes associated with upregulated type I interferon signaling. Nat Genet 46:503-509
60. Rice GI, Kasher PR, Forte GM, Mannion NM, Greenwood SM, Szynkiewicz M et al (2012) Mutations in ADAR1 cause Aicardi-Goutières syndrome associated with a type I interferon signature. Nat Genet 44:1243-1248
61. Rice T, Zheng S, Decker PA, Walsh KM, Bracci P, Xiao Y et al (2013) Inherited variant on chromosome 11q23 increases susceptibility to IDH-mutated but not IDH-normal gliomas regardless of grade or histology. Neuro Oncol 15:535-541
62. Takanohashi A, Prust AM, Wang J, Gordish-Dressman H, Bloom M, Rice GI et al (2013) Elevation of proinflammatory cytokines in patients with Aicardi-Goutières syndrome. Neurology 80:997-1002
63. Van Heteren JT, Rozenberg F, Aronica E, Troost D, Lebon P, Kuijpers TW (2008) Astrocytes produce interferon-alpha and CXCL10, but not IL-6 or CXCL8, in Aicardi-Goutières syndrome. Glia 56:568-578
64. Wang Q, Li L, Wang X, Liu H, Yao X (2014) Understanding the recognition mechanisms of Zα domain of human editing enzyme ADAR1 (hZα(ADAR1)) and various Z-DNAs from molecular dynamics simulation. J Mol Model 20:2500
65. Weller M, Weber RG, Willscher E, Riehmer V, Hentschel B, Kreuz M et al (2015) Molecular classification of diffuse cerebral WHO grade II/III gliomas using genome- and transcriptome-wide profiling improves stratification of prognostically distinct patient groups. Acta Neuropathol 129:679-693

66. Zhang L, Yang CS, Varelas X, Monti S (2016) Altered RNA editing in 3' UTR perturbs microRNA-mediated regulation of oncogenes and tumor-suppressors. Sci Rep 6:23226

Figure legends

Fig. 1 Germline alterations in the AGS genes *ADAR* and *RNASEH2B* in families with glioma and prostate cancer. **a** Pedigree of family 1 and segregation of *ADAR* and *RNASEH2B* germline alterations detected by WES. Patients III.2 and III.3 each diagnosed with *IDH1*-mutant anaplastic astrocytoma of WHO grade III and their father II.2 affected by a prostate carcinoma are simultaneously heterozygous for rare variants in *ADAR* and *RNASEH2B*. The *ADAR* variant is a known AGS mutation, while the *RNASEH2B* variant is novel. All tested family members carrying both variants were affected by cancer. The paternal great-uncle who died from prostate carcinoma, and the grandmother who died from an adrenal tumor were unavailable for genetic testing. M1: *ADAR*,c.577C>G;p.(P193A), M2: *RNASEH2B,*c.495G>T;p.(K165N). Asterisks indicate patients in whom WES analysis was performed. **b** Pedigree of family 2 and segregation of the germline *RNASEH2B,*c.529G>A;p.(A177T) (M3) variant, a known AGS mutation. Patient II.2 affected by a glioblastoma of WHO grade IV carried the *RNASEH2B* mutation, while a mutation carrier's son diagnosed with myelodysplastic syndrome was unavailable for genetic testing. **c-f** *ADAR*,c.577C>G;p.(P193A) (M1) and *RNASEH2B,*c.529G>A;p.(A177T) (M3), two known AGS mutations, were also detected in the germline (non-neoplastic tissue) and tumor of glioblastoma patients in families 3 and 4 as well as in the germline (non-neoplastic tissue) and tumor of prostate carcinoma patients in families 5 and 6. Question marks indicate that it is unknown whether an individual was affected by a tumor or not.

Fig. 2 Structural changes in the Zα domain of ADAR P193A variant compared to wildtype (WT) protein detected during molecular dynamics (MD) simulations destabilize Z-DNA binding. **a** The ADAR P193A missense variant in the β-wing leads to an increased structural flexibility of the protein, in particular of the Z-DNA/Z-RNA binding β-wing, during MD simulations (indicated by brownish vectors on the Cα atoms). The starting structure of the ADAR Zα domain is shown as green colored cartoon representation, the maximal displacement of the structure along the MD trajectory as transparent cartoon, and the bound Z-DNA as wheat colored cartoon representation. The duplex ADAR Zα domain and Z-DNA, which were part of the simulation system, are

displayed as white silhouette (not shown in **c** and **d**). **b** Difference root mean square fluctuation (RMSF) diagram (WT – P193A) averaged over the amino acid residues, showing the increased fluctuations of the P193A variant as compared to wildtype. **c** Snapshots of the wildtype ADAR MD trajectory. The Z-DNA binding area remains stable and well-pronounced over the simulation time. Only minor changes are detectable in the protein and Z-DNA along the trajectory. **d** Snapshots of the ADAR P193A variant simulation. Larger conformational changes occur in the Zα domain, which appear to destabilize Z-DNA binding. Note the marked conformational changes of the Z-DNA. The Zα domain is shown as a green surface with the position of P193 highlighted in gold, and the Z-DNA as a wheat colored cartoon representation (**c** and **d**).

Fig. 3 RNASEH2B mutant proteins increase double-strand DNA damage and impair ribonucleotide removal from genomic DNA. **a** *Rnaseh2b*$^{-/-}$ MEFs transiently transfected with constructs expressing Rnaseh2b (Rh2b) p.(K162N) or p.(A174T) mutants showed a reduced DNA damage rescue, i.e. a significantly higher percentage of *Rnaseh2b*$^{-/-}$ MEFs with more than five γH2AX DNA damage foci was observed, than after wildtype Rnaseh2b re-expression (mean ± SD for n=4 independent experiments). **b** In human fibroblasts from patient II.2 of family 2 carrying the *RNASEH2B,*c.529G>A;p.(A177T) variant, significantly more nuclei harbored 1-3 γH2AX foci as compared to four control fibroblast cell lines, indicating increased double-strand DNA damage (mean ± SD for n=3 independent experiments). Representative images of stained fibroblast nuclei are shown. **c** Genomic DNA from *Rnaseh2b*$^{+/+}$ MEFs, *Rnaseh2b*$^{+/-}$ MEFs and transiently transfected *Rnaseh2b*$^{-/-}$ MEFs was analyzed on an alkaline agarose gel to estimate sensitivity to recombinant RNase HII enzyme as a measure of ribonucleotide excision repair and DNA integrity. **d** Densitometric evaluation of high molecular weight genomic DNA bands from (**c**) revealed a decreased rescue of *Rnaseh2b*$^{-/-}$ genomic RNase HII mediated DNA fragmentation reflecting a higher ribonucleotide content when expressing Rnaseh2b mutants versus wildtype (mean ± SD for n=3 independent experiments). *, $p < 0.05$; **, $p \leq 0.01$; ***, $p \leq 0.001$ (Student's *t* test).

Fig. 4 Glioma patients with rare *ADAR* or *RNASEH2B* variants and their tumors recapitulate features of the AGS type I interferonopathy. (**a-d**) Glioma patients with rare *ADAR* or *RNASEH2B* variants show hallmark pathologic brain features of AGS patients. White matter hyperintensity on T2-weighted magnetic resonance imaging of patient II.2 of family 2 indicates leukoencephalopathy, and the widened sulci indicate bifrontal lobe atrophy (asterisks) (**a**). HE stained tissue sections reveal several large calcifications (arrows) in the glioma of patient III.2 of family 1 (**b**; scale bar: 300µm), and one small calcification in the non-neoplastic brain tissue of patient II.2 of family 2 (**c**; scale bar: 60µm). Tumor or brain calcifications of other patients are summarized in Supplementary Tables 10, 11, and shown in Supplementary Fig. 5. The calcification score was elevated in gliomas with (n=6) versus without (n=5) rare *ADAR* or *RNASEH2B* variants (mean ± SD) (**d**). **e-h** IFNA6 immunoreactivity in a representative glioma without *ADAR* or *RNASEH2B* variants (**e**: tumor Gb6) and two representative gliomas with *ADAR* or *RNASEH2B* variants (**f**: tumor Gb9; **g**: glioma from patient III.2 of family 1); scale bar: 60µm. The IFNA6 expression was significantly higher in gliomas with (n=6) versus without (n=5) *ADAR* or *RNASEH2B* variants (mean ± SD) (**h**). **i-l** Immunostaining of type I IFN-inducible CXCL10 in a representative glioma without *ADAR* or *RNASEH2B* variants (**i**: tumor Gb19) and two representative gliomas with *ADAR* or *RNASEH2B* variants (**j**: glioma from patient III.3 of family 1; **k**: tumor Gb16); scale bar: 60µm. Gliomas with *ADAR* or *RNASEH2B* variants (n=6) showed significantly higher CXCL10 scores as compared to gliomas without *ADAR* or *RNASEH2B* variants (n=5) (mean ± SD) (**l**). **m** Glioma patients with rare *ADAR* or *RNASEH2B* variants (filled black symbols; n=3) show significantly increased transcript levels of ISGs *IFI27* (circles), *IFIT1* (squares) and *RSAD2* (triangles) in whole blood normalized to *18S* expression levels versus controls (unfilled symbols; n=20). Scatter plots show RQ values on a $\log_{10}$-scale for each individual (mean for n=2 independent experiments performed in triplicate, red lines indicate the mean value of each group). Given are significance levels calculated using two-tailed Student's *t* test. The expression differences between patients and controls remain significant after correcting for multiple testing [6]. WT, wildtype *ADAR* and *RNASEH2B*; mut, mutant *ADAR* and/or *RNASEH2B*; pts, patients; *, $p < 0.05$; **, $p \leq 0.01$; ***, $p \leq 0.001$ (Student's *t* test).

Fig. 5 ISG expression induced by *ADAR* and *RNASEH2B* variants via IRF3 activation is suppressed by JAK1/2 inhibitor Ruxolitinib. **a** Transcript levels of ISGs *IFI27*, *IFIT1*, and *RSAD2* were significantly enhanced upon ADAR p.(P193A) mutant versus wildtype ADAR, and RNASEH2B p.(K165N) and p.(A177T) mutants versus wildtype RNASEH2B expression in LN-229 cells (mean ± SD for n=3 independent experiments performed in triplicate). **b** Nuclear IRF3 accumulation was detected in a significantly higher percentage of LN-229 cells upon expression of ADAR and RNASEH2B mutants as compared to wildtype ADAR and RNASEH2B by immunofluorescence (mean ± SD for n=3 independent experiments). **c** Images show the inhibiting effect of wildtype ADAR on nuclear IRF3 accumulation that is not detected upon expression of ADAR p.(P193A) mutant (more images are shown in Supplementary Fig. 10). **d** Treatment with 1 µM JAK1/2 inhibitor Ruxolitinib versus DMSO control abolished induction of *IFI27*, *IFIT1*, and *RSAD2* transcript levels upon expression of mutant ADAR and RNASEH2B in LN-229 cells (mean ± SD for n=3 independent experiments performed in duplicate). *, $p < 0.05$; **, $p \leq 0.01$; ***, $p \leq 0.001$ (Student's *t* test).

figure 1

Click here to download figure Beyer et al_Figure 1_600dpi.tif

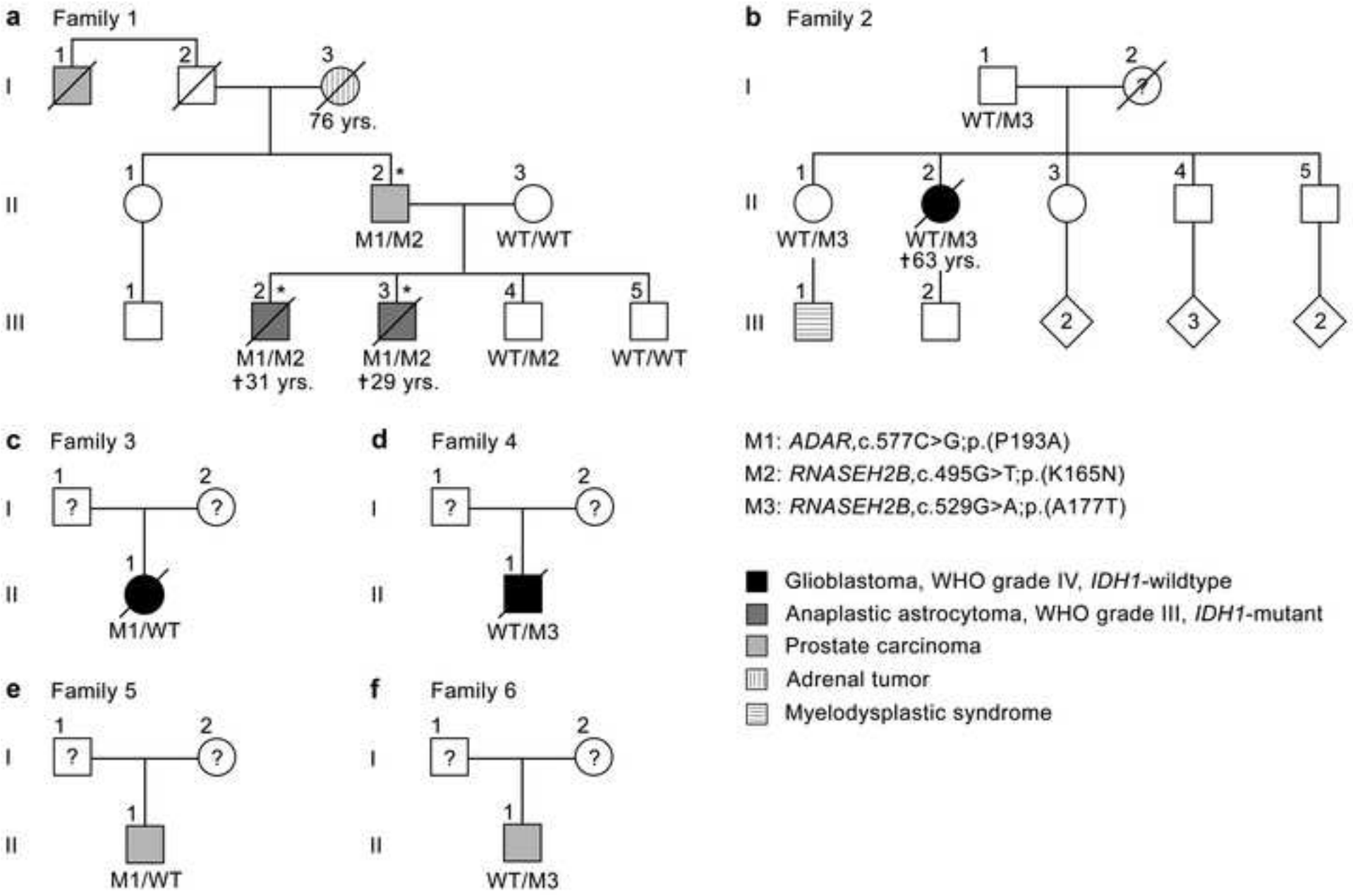

figure 2

Click here to download figure Beyer et al_Figure 2_600dpi.tif

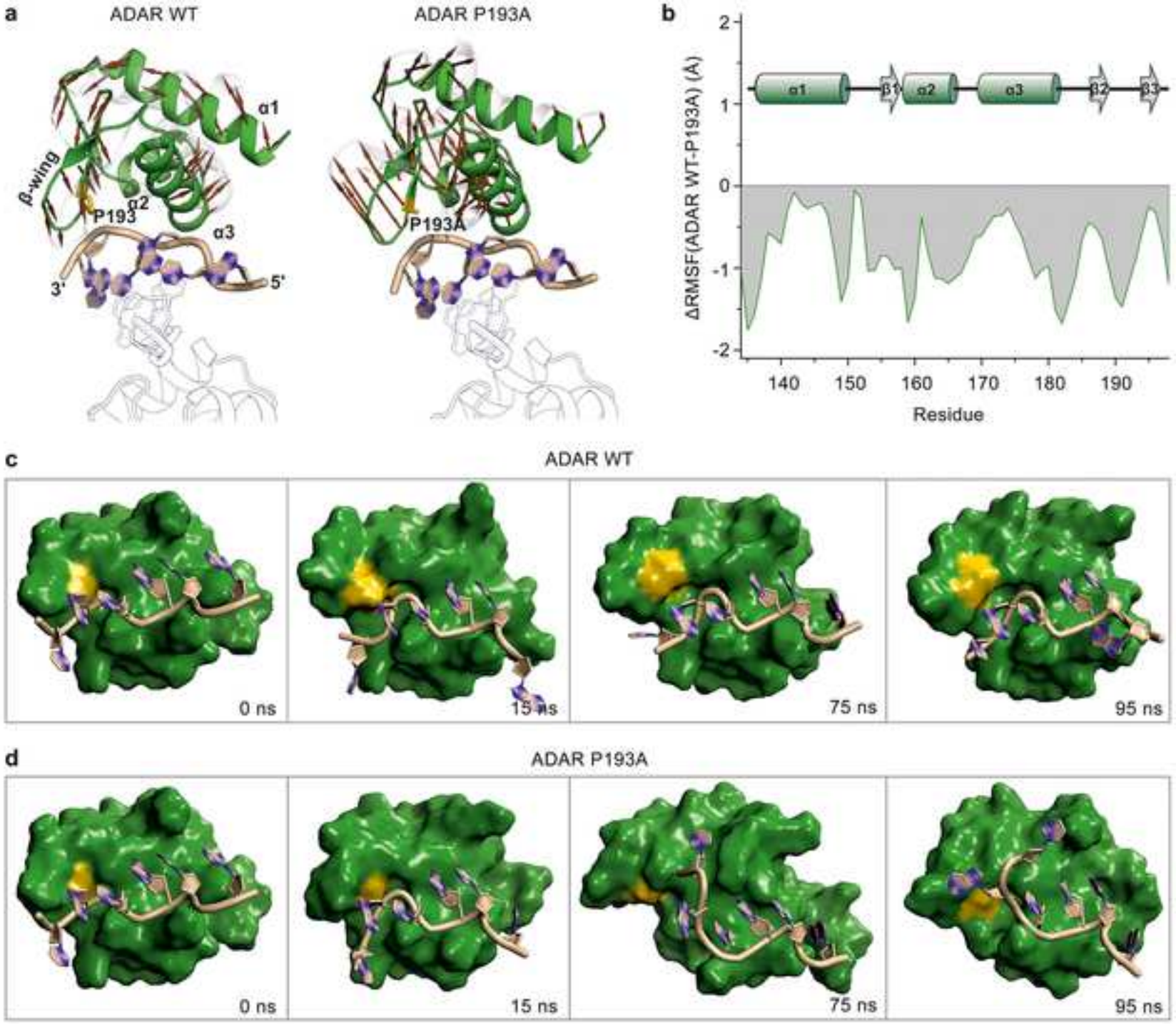

figure 3

Click here to download figure Beyer et al_Figure 3_600dpi.tif

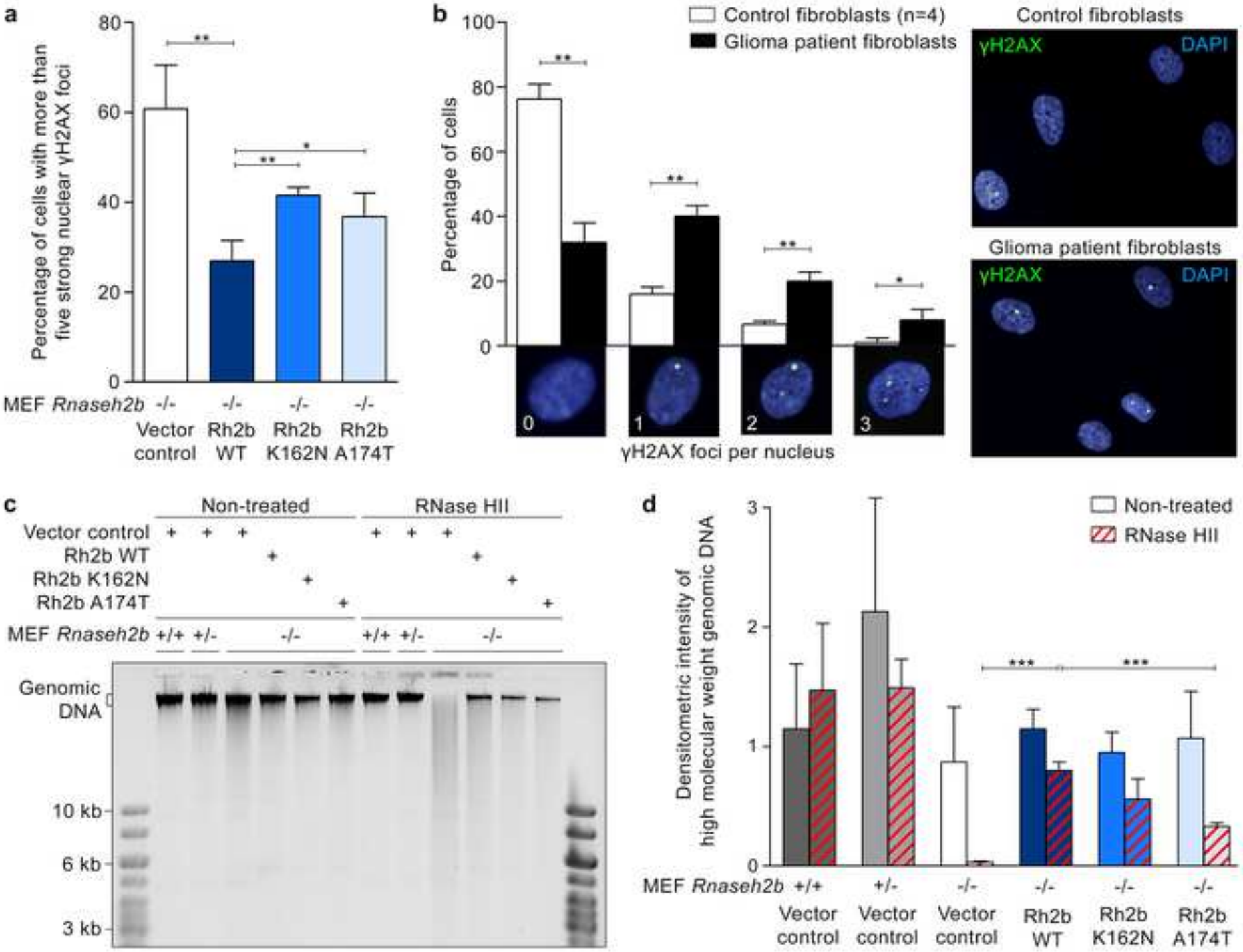

figure 4

Click here to download figure Beyer et al_Figure 4_600dpi.tif

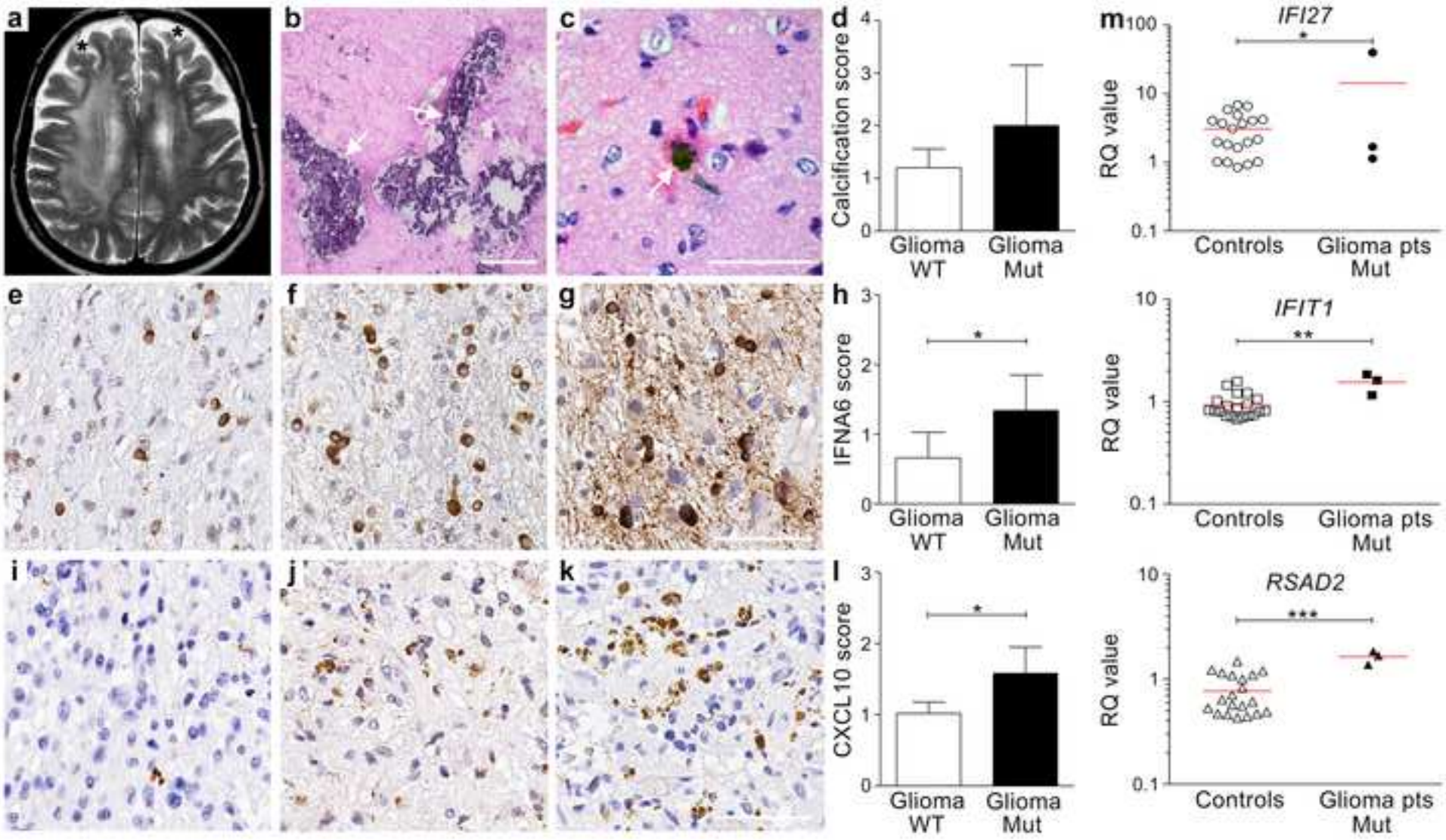

figure 5

Click here to download figure Beyer et al_Figure 5_600dpi.tif

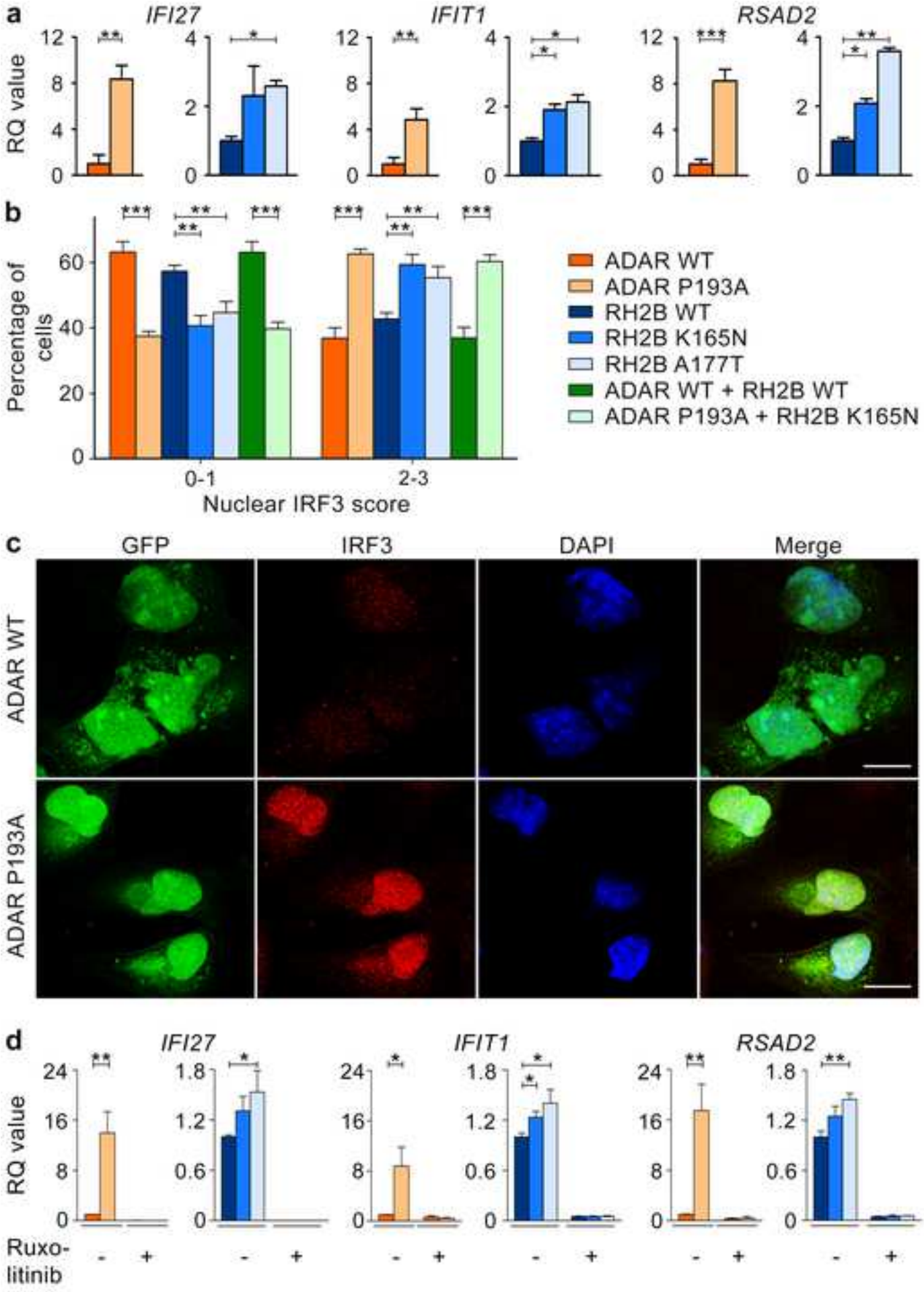

Click here to access/download
electronic supplementary material
Beyer et al Supplementary material.pdf

Click here to access/download
electronic supplementary material
Beyer et al Supplementary Table 2.xlsx

Click here to access/download
electronic supplementary material
Beyer et al Supplementary Table 4.xlsx